Disclaimer: This is not the final version of the article. Changes may occur when the manuscript is published in its final format.

Dynamic Virtual Tumor Cells Powered by Spatial Omics for Translational Oncology

Ke Li[1], Yu Liu[2], Guangzhao Huang[1], Ruohan Zhai[3], Chunjie Li[1*]

1. State Key Laboratory of Oral Diseases & National Center for Stomatology & National Clinical Research Center for Oral Diseases & Department of Head and Neck Oncology, West China Hospital of Stomatology, Sichuan University, Chengdu 610041, Sichuan, China.

2. Faculty of Dentistry, The University of Hong Kong, Hong Kong.

3. State Key Laboratory of Oral Diseases & National Clinical Research Center for Oral Diseases & Department of Cariology and Endodontics, West China Hospital of Stomatology, Sichuan University, Chengdu 610041, Sichuan, China.

*: Correspondence to Prof. Chunjie Li, email: lichunjie@scu.edu.cn

Abstract

Cancer is a serious health problem worldwide. The treatment resistance and variability in clinical outcomes are both challenges for oncology. The tumor microenvironment (TME) plays a significant role in tumor development, treatment response, and spatial heterogeneity. These characteristics vary among different cancer types, patients, and tumor regions. Traditional methods in oncology have not been able to deeply understand the complexity of these interactions without considering spatial factors. In recent years, the development of spatial omics has made significant progress. This technology can analyze gene activity, protein expression, and cell communication within tissues at the same time, providing a deeper understanding of the TME.

This review explores how spatial omics technologies can help connect molecular profiling with clinical applications. We particularly focus on the concept of a "virtual tumor ecosystem." We discuss how spatial omics data can be integrated with computational models to build dynamic, patient-specific digital simulations. These virtual tumor organs can mimic actual tumor behavior and predict treatment responses. The ability to use a patient's own spatial data to simulate therapies and predict drug resistance represents a significant advance in precision cancer medicine. The virtual tumor ecosystem can link spatial omics data with the treatment outcomes of patients, and is expected to enhance the level of personalized cancer treatment. This review summarizes the latest progress in using spatial omics technology to construct cancer models. We also discuss the main challenges faced by this method and its future development prospects. We are aiming to promote the clinical application of related research results and to develop more effective treatment plans for each patient.

Keywords

spatial omics; tumor microenvironment (TME); virtual tumor; digital twins; personalized cancer therapy; precision oncology; computational oncology

1. Introduction

Cancer is a major health problem around the world. Doctors often find that treatments stop working, and patients can have very different results. This makes working with the disease hard. Inside a tumor, there is a special environment. This tumor microenvironment (TME), is made of non-cancerous cells. These cells touch the cancer cells at the tumor's center and its edges. What the TME looks like changes based on the type of cancer. It is also different from one person to another. A single patient can even have different TME makeups in different tumors. Tumors also have their own natural variety inside them. This variety comes from two things. First, cancer cells develop different genes as they grow and multiply. Second, the cancer cells react with the body's immune cells and other supporting cells. All of this creates the different features doctors see in different parts of a single tumor[1, 2]. More and more studies show the physical layout of the TME is a big part of how well treatments work or why they fail. Doctors sort tumors by these features, calling them "immune hot," "immune cold," or "immune exclusion." These names show that the small areas where cells live, their tiny three-dimensional niches, are not just labels. They are directly connected to why a treatment works[3, 4].

Using just 2D sample cannot rebuild the full picture of how cancer cells grow in 3D or how immune cells are arranged. Older methods, which look at many cells mixed together or at single cells, always lose the information about where things are. To prepare a sample, scientists break the tissue apart. This process removes all information about where each cell originally sat. Even the most advanced tests for genes or proteins only give a view of a single moment. This kind of data cannot show how a treatment changes the environment over time. It also cannot explain the big differences seen from one patient to another. This missing information, which we call the spatial-temporal-individualization (STI) divide, is a major obstacle to precision oncology[5].

In the most recent years, spatial omics has rapidly emerged as a technological framework capable of quantitatively assessing RNA and protein states in intact tissues. Advances in high-throughput sequencing and imaging technologies make it possible for identifying and characterizing these aspects of heterogeneity. Spatial omics becomes a pivotal tool for understanding tumor heterogeneity and TME interactions[5-10]. Systematic study of the molecular phenotypes of millions of cells within a tissue context can be conducted, bridging the limitations of both histology and single-cell omics. Platforms such as Visium and CosMx offer transcriptomic-

level resolution, while techniques like imaging mass spectrometry (CODEX) and multiplex immunofluorescence enable high-dimensional spatial protein mapping[11]. By integrating tissue clearing and 3D imaging workflows, these technologies have extended spatial omics into the realm of 3D analysis[12]. Compared to traditional bulk and single-cell omics, spatial technologies enable the concurrent analysis of cell types, neighborhood relationships, and functional pathways in situ within tissues, and are progressively expanding to integrate multimodal measurements[13, 14].

If doctors only use maps that just show where things are, it is hard to use them in the clinic. For them to really work in the clinic, doctors need to turn that information into working models that show how things change and why. These models must also be able to change and grow for each patient. This leads to the concept of the virtual tumor cell (VTC) that integrates spatial omics evidence into a computational, interactive, and iteratively updatable digital twin framework[15, 16]. Building on VTCs, we assemble virtual tumor organs (VTOs). Tumor-specific virtual organs emphasize translational medical applications. They can integrate multi-scale data through frameworks such as graph networks and Bayesian methods, simulating drug or immunotherapy interventions within a virtual environment. As new patient samples are input, these models continuously refresh, offering the potential to truly close the loop of "evidence→VTC→decision"[17].

Building virtual cells, and then virtual organs, with the aid of spatial omics evidence updating and upgrading the loop based on patient-level data, offers an actionable pathway to transform phenomena into decisions. First, spatial evidence can more directly link the structure of the microenvironment with therapeutic outcomes[18, 19]. Secondly, virtual representations enable the simulation of dynamic processes, such as clonal competition, immune infiltration, and drug diffusion, which are not directly observable, building upon the foundation of static descriptions[20, 21]. Thirdly, patient-level updates transform the model from a research tool into a clinical instrument, capable of supporting biopsy site selection, treatment regimen prioritization, and resistance risk prediction[22]. These principles collectively form what we refer to as the virtual tumor ecosystem (VTE). (See Box 1 for formal definitions and the hierarchical framework)

Virtual Tumor Cell (VTC) – the microscopic unit. The fundamental computational unit representing the molecular state and behavior of an individual cell. VTCs are initialized by high-dimensional spatial omics data and can simulate cellular responses to perturbations using generative foundation models.

Virtual Tumor Organ (VTO) – the mesoscopic assembly. A spatially resolved, multicellular assembly of VTCs that recapitulates tissue architecture, cell-cell interactions, and microenvironmental gradients in silico. VTOs simulate emergent properties of the tumor mass within a specific tissue context.

Virtual Tumor Ecosystem (VTE) – the systemic integration. The overarching, patient-specific digital twin framework that integrates VTOs with multi-scale clinical data streams, such as longitudinal imaging, treatment history). It represents the translational horizon aiming to enable dynamic simulation and real-time therapeutic decision-making.

Box 1: Terminology and Hierarchy of the Virtual Tumor Framework

In this review, we propose that the integration of spatial omics with VTCs and VTOs is an inevitable evolution in the development of precision oncology. By operationalizing the STI gap, assembling VTEs, and embedding them into the clinical decision-making loop, this approach holds significant potential. I This approach can change how useful spatial data is in the clinic, help move findings from molecular tests into treatment plans faster, and create new ways to get past drug resistance and give each person a therapy made just for them (Figure 1).

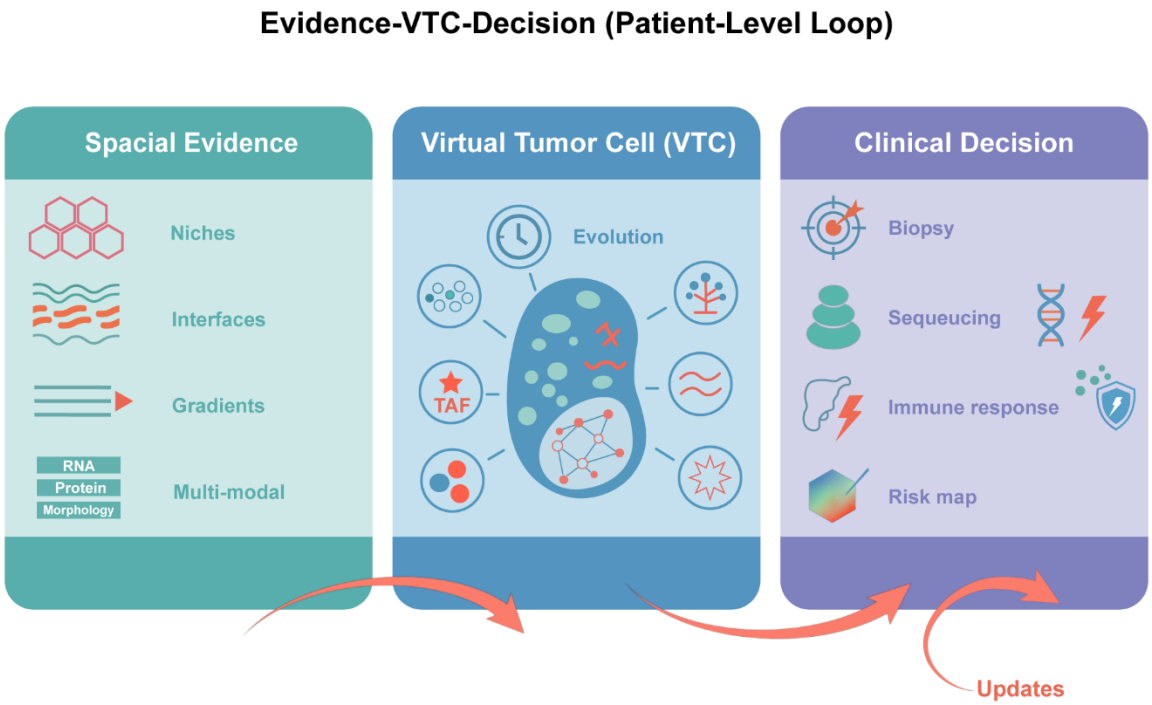

Figure 1. Evidence-VTC-Decision (Patient-Level Loop). This figure illustrates the iterative process from spatial evidence collection, through the creation of a VTC, to clinical decision-making, with continuous patient-level updates driving personalized treatment strategies.

2. Spatial Omics Technology Supports the Spatial Tumor Ecosystem Framework

2.1 Spatial Omics Technology

Spatial omics technology has shifted from traditional molecular-level analysis to capturing the spatiotemporal dynamics within tissue microenvironments. In recent years, with advancements in high-resolution imaging and computational algorithms, the field of spatial omics has rapidly developed, progressing toward higher throughput, lower noise, and stronger integration capabilities[13]. In oncology, these technologies have unveiled the core mechanisms of cellular heterogeneity and spatial interactions, driving the shift from descriptive studies to predictive models. Table 1 lists the representative spatial omics technologies.

Table 1: Comparative Landscape of Spatial Omics Technologies

Technology Category	*Core Technology Principle*	*Representative Platforms / Assays (Year)*	*Key Features*	*Resolution*	*Throughput*	*Panel Size/Plex*	*Sample Compatibility*	*Application Scenarios*	*References*
Spatial transcriptomics	Multiplexed ISH	seqFISH (2014) / seqFISH+ (2019)	Ultra-high resolution enabling organelle-level transcript localization.	Subcellular/Single molecule	Low (limited by imaging time)	10,000+ genes	FFPE (partial) & FF	Basic research: chromatin structure, nuclear RNA localization, single-cell gene expression heterogeneity.	
		Xenium (2023) /Xenium Prime (2024)	High sensitivity; Prime version significantly improves imaging speed and whole-slide scanning.	Subcellular, ~200nm	High	5,000+ genes / 18,000+ WTA	FFPE & FF	Detailed TME mapping, rare cell type localization, gene signature validation in translational research.	23-26
		MERFISH (2015)/MeERSCOPE Ultra (2024)	High detection efficiency and molecular localization precision; Ultra version supports larger imaging area.	Subcellular, ~100nm	Medium -high (Ultra)	500-1000 genes, expandable	FFPE & FF	Brain atlas construction, detailed cell atlas, subcellular RNA distribution studies.	
	In situ sequencing	Fluorescent In Situ Sequencing (2014)	Visualizes individual RNA transcripts.	Subcellular	Low	Targeted, ~5,000 genes / Whole transcriptome	Fixed Cells & Tissues	Subcellular RNA localization, analysis of intra-cellular gene expression heterogeneity.	
		STARmap (2018)	Enables 3D imaging. Preserves spatial context in intact tissue.	Single cell and Subcellular	Medium -high	Highly targeted (hundreds to thousands of genes)	Intact Tissues	3D single-cell transcriptomics in intact tissues, brain structure mapping.	26-30
		ExSeq (2021)	Uses physical/chemical tissue expansion (hydrogel) for sequencing within	Nanoscale/Super	Low	Targeted/Untargeted	Intact	Nanoscale spatial transcriptomics,	

			the enlarged space.	Sequencing			biological systems	subcellular structure analysis.	
	In situ capture	Slide-seq V2 (2021)	High sensitivity; improved capture efficiency vs. V1.	~10μm (near-single-cell)	High	Whole Transcriptome	FF	Retrospective analysis, high-resolution tissue mapping.	
		seq-scope (2021)	Enables microscope-level examination of spatial transcriptomes.	0.5μm spot-to-spot resolution	High	Whole Transcriptome	FF	Study of transcriptome dynamics at organelle level.	
		Stereo-seq V2(2022)/Stereo-seq V3(2025)	Combines large imaging area with high resolution.	Subcellular, ~500nm center-to-center	Very high	Whole Transcriptome	FFPE & FF	Multi-organ tumor metastasis studies, large-sample mapping.	[26, 31, 32]
		Visium-HD (2024)	~25x higher resolution than standard Visium (55μm), with no data gaps.	Subcellular, 2μm squares	Medium -high	Whole Transcriptome	FFPE & FF	Fine-grained TME analysis, retrospective clinical pathology studies, gene expression mapping in fine anatomical structures.	
	Slide-tags	slide-tags (2023)	Spatial barcoding for single nuclei, automatic cell segmentation.	less than 10 μm	High	Whole Transcriptome	FF	Immune microenvironment and ligand-receptor interactions, 3D digital reconstruction.	[33]
Spatial proteomics	Mass-spectrometry imaging cytology	IMC (2014)/IMC Hyperion Xti (2023)	Uses metal tags instead of fluorophores, minimal signal crosstalk, very low background noise.	Subcellular	Low-high	30-50 plex	FFPE＆ FF	Immune checkpoint analysis, TIME neighborhood subtype classification.	[34, 35]
		MIBI-TOF (2014)	High sensitivity and wide dynamic range.	Subcellular	Low- Medium	40–50 plex	FFPE	Structured immune microenvironment analysis.	

	Cyclic fluorescence multiplexing	CODEX (2018)/PhenoCycler-Fusion	Relies on cyclic hybridization and imaging.	Subcellular	Medium -high	100+ plex	FFPE & FF	Large cohort studies, single-cell protein interaction network construction.	[36, 37]
		COMET (2023)	High automation and very short cycle times.	Subcellular	Very High	100+ plex	FFPE	Intra-tumoral clonal structure, spatial genetic heterogeneity, cancer evolution.	
Spatial genomics	Microdissection-based	slide-DNA-seq (2021)	Built on Slide-seq; maps clonal evolution within tumors	10μm	Medium -high	Whole genome/Targeted Panel	FFPE	Intra-tumoral clonal structure, spatial genetic heterogeneity, cancer evolution.	[38-40]
		LCM-WGBS (2018)	Performs whole-genome bisulfite sequencing on microdissected samples.	ROI-level	Low	Whole Genome Methylation	FFPE & FF	Methylation profiling of specific tissue regions.	
		LCM-RNA-seq (2013)	Traditional sequencing post-microdissection; highly customizable region selection.	ROI-level	Low	Whole transcriptome/Targeted	FFPE & FF	Validation of region-specific gene expression from spatial transcriptomics discoveries.	
		Geo-seq (2016)	High precision, suitable for trace amounts of tissue.	Single to few-cell level	Medium -high	Whole transcriptome	FF	Early embryo development, spatial transcriptomics of trace amounts of rare cells.	

Spatial epigenomics	In situ chromatin profiling	scSpatial-ATAC (2021)	Combines ATAC-seq with spatial barcoding for in situ chromatin accessibility profiling.。	Single-cell, ~10μm	High	Genome-wide open chromatin regions	FF	Spatial mapping of regulatory elements in development/disease, identification of cell-type-specific enhancers.	[41-43]
		Spatial-CUT&Tag (2021)	Combines CUT&Tag with spatial technology for in situ detection of histone modifications or TF binding.	10-55μm (platform-dependent)	Medium	Targeted epigenetic marks	FF	Spatial epigenetic state analysis, epigenetic regulation of cell fate decisions.	
		sciMAP-ATAC (2022)	Microfluidics-based combinatorial indexing; retains partial spatial information.	Cell-cluster level	High	Genome-wide open chromatin regions	Fresh nuclei	Medium-throughput spatial epigenomic atlas construction.	
Spatial metabolomics / lipidomics	Mass spectrometry imaging	MALDI-MSI (2000s/2021)	Most established spatial metabolomics technique; label-free, directly detects metabolites/lipids.	5–100μm / Sub-micron, <5μm (with OTCD)	Medium	Untargeted, hundreds to thousands of metabolites	FFPE (partial) & FF	Tumor metabolic reprogramming, spatial distribution of drugs and their metabolites, neuroscience.	[44-46]
		DESI-MSI (2000s)	Operates under ambient conditions, requires no matrix, suitable for real-time analysis.	50-200μm	Medium	Untargeted, hundreds of metabolites	Untreated tissue sections	Intraoperative real-time tissue analysis, spatial lipid-metabolism profiling.	
		ToF-SIMS (1980s)	Extremely high surface sensitivity; detects elements and small inorganic/organic molecules.	<1μm	Low	Elements, small molecules, lipid fragments	Various solid samples	Subcellular elemental distribution, drug-penetration studies, material-surface analysis.	
Combination / Multimodal integration	Sequential multimodal	Visium + IHC/IF	H&E/IHC/IF imaging first, followed by Visium sequencing on the same tissue region.	ROI-level / near single-cell	Medium	RNA + Protein (~10-40 markers)	FFPE & FF	Direct correlation of gene expression with key protein markers.	[47-49]
		Xenium + IF/H&E	High-plex RNA in situ detection and protein/morphology imaging on the same slide.	Subcellular	High	RNA (5000+) + Protein (~4-10 markers)	FFPE & FF	High-precision multi-omics co-localization.	

		CODEX × RNAscope	Multiplexed protein imaging followed by targeted RNA in situ hybridization.	Subcellular	Medium-High	Protein (100+) + RNA (a few targets)	FFPE	Deep profiling of cellular functional states (protein) and key gene expression.	1
	Simultaneous multimodal	DBiT-seq (2020)	Simultaneously captures RNA and protein via microfluidic barcoding (oligonucleotide-tagged antibodies).	10–25μm	Medium	RNA + Protein (a few to tens of markers)	FF	Matched transcriptome and proteome data from the same cells.	
		GeoMx (2019)	Non-destructive; tissue section can be used for subsequent staining.	Multicellular, ROI-level	High sample-throughput	Whole transcriptome (18,000+ RNA) + High-plex protein (100+)	FFPE & FF	Clinical biomarker discovery, regional analysis of tumor/immune microenvironment, retrospective pathology studies.	26, 50, 51
		CosMx SMI 2.0 (2024)	Dual RNA and protein detection; version 2.0 significantly increases RNA coverage.	Single cell and subcellular, ~0.5-1.2μm	High-plex	6,000+ RNA (up to whole-transcriptome ~18k plex) + 64-plex protein	FFPE & FF	Studying complex ligand–receptor interactions within tissues.	
		G4X (2025)	Enables in situ multi-omics detection, allowing for the simultaneous measurement of RNA and proteins in a single run.	Single molecule	High	RNA: ~300-500 genes (Targeted). Protein: ~15-18 markers.	FFPE	Supports 3D spatial multi-omics analysis through serial sections.	

2.1.1 Spatial transcriptomics

Spatial transcriptomics unveils gene expression and cellular behavior within the TME by mapping gene expression profiles on tissue sections and correlating the gene data with spatial coordinates[8, 52]. Early technologies utilized array-based transcript capture, but their resolution was limited. Modern high-resolution techniques combine imaging and sequencing methods, such as in situ sequencing with nanoscale probes, achieving transcript localization at subcellular resolution and preventing the loss of spatial information[53, 54]. By registering consecutive tissue slices to reconstruct 3D transcriptional spatial information and integrating temporal data, dynamic spatial transcriptomics has emerged as an extension of spatial omics[55]. New deep learning models contribute to optimizing these technologies at the technical level. Advances in artificial intelligence (AI)-assisted real-time transcriptome reconstruction, combined with neural network simulations of treatment-induced transcriptional remodeling, have enhanced the ability to dynamically track changes from baseline to the resistance stage[56].

2.1.2 Spatial proteomics

Spatial proteomics addresses the limitations of spatial transcriptomics by directly providing spatial distribution information of functional proteins. Through mass spectrometry imaging (MSI) and cyclic labeling strategies, spatial proteomics enables the simultaneous quantification of dozens to hundreds of proteins, overcoming the multiplexing limitations of traditional immunofluorescence techniques[57]. In dynamic spatial proteomics, enhanced resolution imaging techniques allow for tracking protein reprogramming during treatment. Xu et al. utilized Panoramic Spatial Enhanced Resolution Proteomics to monitor gradient changes of key proteins such as epidermal growth factor receptor in tumors, predicting the expansion of drug-resistant clones[58, 59].

2.1.3 Other spatial omics technologies

Other omics layers, such as metabolomics and epigenomics, are expanding the research dimensions of spatial omics[60]. Spatial epigenomics explores the spatial distribution of epigenetic modifications, such as DNA methylation and histone modifications, revealing how these modifications function in different tissue or cellular environments[61].

Spatial metabolomics, through imaging mass spectrometry, captures metabolite gradients, such as the accumulation of lactate in hypoxic regions, shedding light on the spatial heterogeneity of tumor metabolic reprogramming[44, 62]. The incorporation of Matrix-assisted laser desorption ionization MSI and ion-mobility spectrometry has markedly broadened the detectable repertoire of small molecules and lipids, with substantial gains in sensitivity and resolving power[63, 64]. Extensions of spatial metabolomics such as SpaceM enable high-resolution, subcellular-scale characterization of spatial features[65].

2.1.4 Spatial multi-omics and the integration of multimodal data

Spatial multi-omics technologies capture the distribution of multiple omics layers within tissue space, offering a multidimensional view of cellular behavior and spatial information. By combining spatial transcriptomics with spatial proteomics, researchers can map the metabolic states and epigenetic regulatory networks of tumor-infiltrating immune cells. The integration of spatial multi-omics is further enhanced through data fusion algorithms, such as MultI-modal Spatial Omics developed by Kyle Coleman and soScope developed by Li et al., which improve the resource utilization of spatial omics technologies[66, 67].

Current cutting-edge technologies emphasize cross-modal integration, such as AI-driven alignment algorithms, which enable pre-training across different omics datasets while incorporating spatial analysis for molecular characterization of cells[68]. For instance, the integration of single-cell and spatial resolution spatial multimodal approaches allows for a multidimensional and in-depth understanding of epigenomics, transcriptomics, and/or proteomics molecular information[69]. These technologies have revealed multi-layered interactions in cancer research.

2.2 Spatial Omics–Derived Spatial Signatures and Clinical Oncologic Links

Spatial signature refers to the characteristic spatial pattern or feature set formed by the relationship between cell types, molecular expression, and spatial positioning within tissues or TME. By leveraging spatial signatures, one can interpret multidimensional information on gene expression, spatial location, and intercellular interactions, and, when necessary, integrate this data through 3D serial section registration and cross-modal alignment (Figure 2).

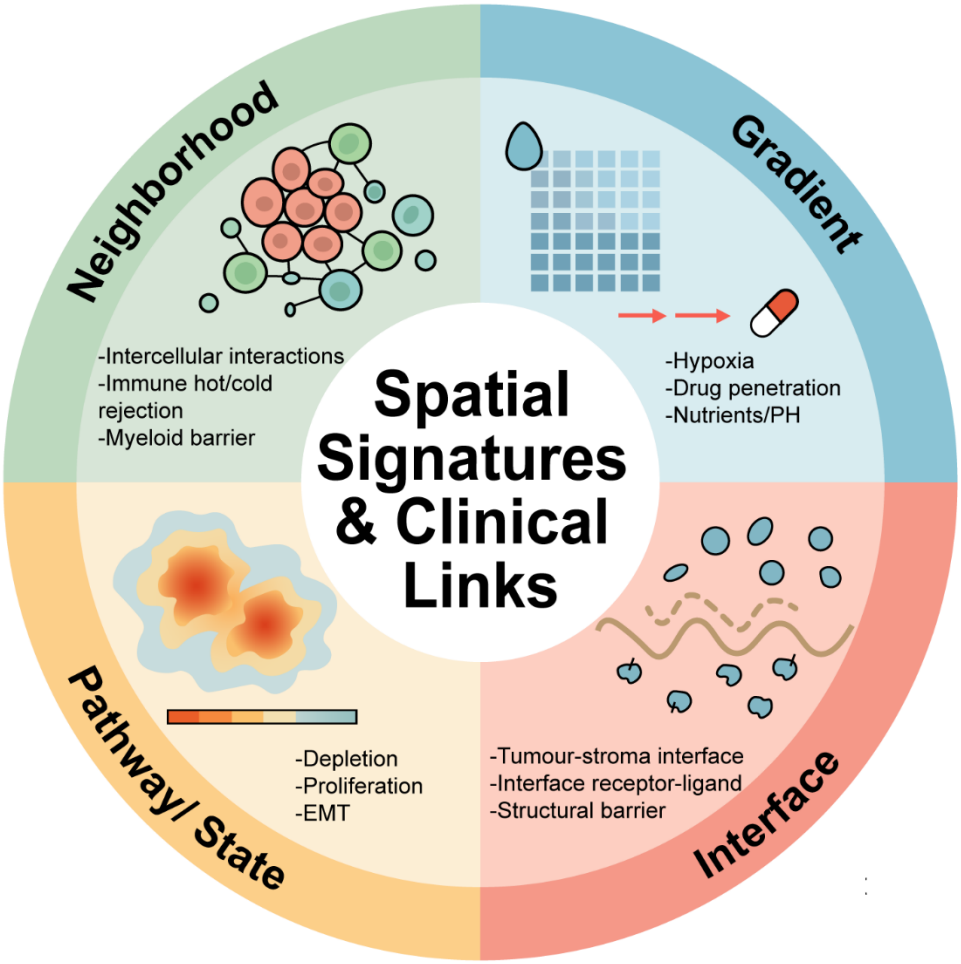

Figure 2. Spatial Signatures and Clinical Links. This figure shows the main spatial signatures and why they matter in the clinic. These spatial features, like how cells interact, how molecules spread out, and the edges between tumor and support tissue, are key to understanding why tumors differ and how they respond to treatment. Doctors use spatial signatures as important clues to make decisions because they give a changing, useful picture of the TME and how it all works together.

2.2.1 Spatial molecular gradient

The gradient phenomena in TME, such as hypoxia, drug penetration, nutrient availability, and pH gradients, create a complex spatial heterogeneity. Gradient signatures map this spatial feature back to tissue geometry, further tracking the coupling between continuous variations and cellular state lineages, clonal landscapes, and immune infiltration[70]. The tumor center and periphery exhibit reproducible pathway stratification, with the

center tending toward metabolic and high-energy states, while the periphery is enriched in inflammation and innate immunity[71]. Greenwald et al. developed a five-layer gradient model, that integrates hypoxia-blood supply-cell states in glioblastoma, combining Visium and CODEX technologies in a cross-modal approach. This study also validated the coherence of internal and external tumor gradients across different scales[72].

By integrating spatial risk maps, gradient signatures can be used to identify phenomena such as drug penetration barriers, resistant ecological niches, and immune exclusion, providing strategies for clinical drug optimization, dose stratification, and therapy sequencing. Research by Natalie Landon-Brace et al. indicates that oxygen gradients can drive an increase in "basal-like" proportions, correlating with gemcitabine resistance[73]. Terrassoux L and others recreated the spatial heterogeneity of treatment response by engineering radial hypoxia and acidification gradients within an extracellular matrix (ECM)-composite microenvironment. Their work successfully characterized the spatial origins of radioresistance, and established a controllable platform for the gradient to resistance phenomenon[74]. Recent advancements in the controllable modeling and visualization of gradients in the TME have provided actionable toolchains to push mechanisms toward clinical applicability. Auxillos et al. developed an integrated microfluidic system capable of generating and monitoring pH gradients in a 3D collagen matrix in real time. This system enables concurrent live-cell imaging and spatial transcriptomics sequencing, thereby offering a continuous mapping from gradient perturbation to spatial transcriptional responses[75]. Meanwhile, MSI directly images the tissue distribution of drugs or metabolites, identifying pharmacokinetic resistance and optimizing dosage and administration paths, while photoacoustic chemical imaging noninvasively and quantitatively monitors pH to predict chemotherapy efficacy[76-78]. Thus, gradient signatures not only quantify spatial phenomena but also serve as spatial trigger points for neoadjuvant/perioperative treatment stratification, facilitating the early identification of low permeability and resistant ecological niches and guiding sequential drug administration.

2.2.2 Cellular neighborhood

Cellular neighborhood signatures characterize "which cells are spatially adjacent and what types of interactions occur between them," while cellular neighborhood analysis divides tissues into several spatial microenvironments (niches), revealing the factors that influence tumor progression and treatment response.

The hot/cold/exclusion framework has become a universal language for immune therapy stratification, where immune hot/cold/exclusion is not merely a difference in cell counts, but rather is determined by the adjacent architecture of immune cells and their functional states[5, 79]. In a 3D context, spatial scoring of immune hot/cold neighborhoods surrounding spatial subclones, based on distance to neighborhood relationships, can more effectively predict patient outcomes and treatment responses[80, 81]. The neighborhood and functional axis of tumor-myeloid-T cells further delineate the foundational typology of "hot" versus "rejected," offering insights into the variability of immune therapies[82]. In the multimodal breast cancer atlas, recurrent immune-stroma-tumor niches were identified, along with a PD-L1/PD-L2^{+} macrophage population linked to clinical outcomes, which form the cellular basis for the hot/rejected classification[83]. Compared to total immune quantity, the combined effects of "location × composition" provide a more robust explanation of prognosis. Zhang et al. confirmed that immune hotspots enriched with effector T cells are located more frequently at accessible tumor peripheries/interfaces rather than deep within the tumor. Notably, they demonstrated that the spatial positioning of these hotspots is more predictive of clinical outcomes than mere effector T cell counts [84] BANKSY, developed by Vipul Singhal, is a machine learning tool that integrates spatial data through a biologically motivated approach, clustering cells into types or tissue domains. It encodes the cellular microenvironment using a pair of spatial kernels, quantifying the gene expression gradients surrounding each cell[14, 85].

Cellular neighborhood signatures provide incremental information that transcends the total and single-indicator approaches. Large cohort studies based on imaging mass cytometry reveal that the spatial organization of cellular neighborhoods and multicellular ecological combinations is not only closely linked to molecular subtypes and somatic alterations but also correlates with prognosis and adverse clinical outcomes. This suggests that the coupling of genomics to ecology can directly manifest as clinical risk phenotypes through the structure of cellular neighborhoods[86, 87].

2.2.3 Inter-domain interfaces

Inter-domain interface signatures focus on the organizational boundaries and material exchange between two ecological or clonal domains. This includes the location, width, and curvature of the interface, the changes in cellular and pathway profiles on either side, and whether specific receptor-ligand axes are enriched at the interface. By combining morphological and molecular segmentation to localize the tumor invasive frontier and

the tumor-stroma boundary, a symbolic distance field is constructed to quantify layering indices, surface roughness, curvature, and cross-boundary interaction flux. These are further assessed for 3D continuity and curvature through nonlinear registration of multiple slices.

Ordered and penetrable interfaces are often associated with higher immune infiltration and better outcomes. In contrast, serrated or highly curved interfaces, accompanied by strong stromal responses and reduced T cell functionality, suggest a synergistic relationship between structural barriers and immune suppression. In Feng et al.'s definition of the tumor-stroma interface band in colorectal cancer, disorganized and accessible tumor-stroma interfaces are linked to stronger immune infiltration and a better response to immune checkpoint blockade. Conversely, ordered, dense barrier interfaces formed by cancer-associated fibroblast-ECM (CAF-ECM) are associated with T cell exclusion and a lack of response[88]. Keren et al.'s study using Multiplexed Ion Beam Imaging in triple-negative breast cancer also demonstrates that the ordered stratification of the tumor-immune boundary and the enrichment of inhibitory axes are significantly correlated with patient prognosis[19].

The ordered stratification of interface structures and the enrichment of immune/suppressive axes are associated with outcomes and treatment responses. In cutaneous squamous cell carcinoma, Andrew L Ji et al. discovered that the tumor frontier exhibits tumor-specific keratin enrichment and is adjacent to the CAF endothelial fibrous-vascular ecological niche, accompanied by Treg-CD8 co-localization and CD8 exclusion immune patterns. This suggests that the coupling of interface structure and immune suppression may form a critical basis for the variability in response and resistance to immune checkpoint inhibitors[89]. The immune microenvironment at the interface and CAF-mediated signaling axes frequently constitute druggable targets. In the invasive frontier of basal cell carcinoma, tumor-derived Activin A, which is encoded by inhibin βA drives ECM remodeling through activin receptor–like kinase 4 on CAFs, indicating the practical feasibility of intervening in these tumor-stroma interface pathways[90]. This interface pattern is also replicated at the spatial protein level in large cohorts and points to the TGF-β/ VEGF axis[91]. A similar matrix-receptor-pathway-transcription factor cascade has been cross-cohort validated in consensus molecular subtype 2-dominated colorectal cancer, further supporting the stratification and potential for intervention in interface signatures[92]. Therefore, interface geometry and interactions not only serve as descriptive morphology but also as priors for neoadjuvant and perioperative treatment responses and spatial trigger points for combination therapies.

2.2.4 Functional state spatialization

Pathway/state signatures characterize the functional states of cells, such as exhaustion, proliferation, epithelial–mesenchymal transition, and stemness, and their associated pathway activities in spatial coordinates. These signatures focus on the spatial layout and co-occurrence/exclusion relationships of these states within the microenvironment. Pathway/State signatures transcribe specific functional states into spatial hotspots or band-like enrichments and their connectivity/self-correlation. A common analytical pipeline begins with calculating state scores using single-sample gene set enrichment analysis, gene-set activity scoring method, or protein composite markers. This is followed by generating spatial heatmaps and quantifying Moran's I/Geary's C, hotspot area, and connectivity. Finally, these spatial features are linked to neighborhoods/interfaces to determine whether they represent structural hotspots[93].

Zhang et al.'s study found that immune hotspots within tumors are not high-functioning immune activation zones. Instead, they are associated with upregulated B cell enrichment signals, a decrease in the $CD8^+$/Treg ratio, and reduced T-B interaction diversity, presenting an immune-suppressive state profile. This was predicted as the "spatial position of the hotspot" driving the functional state rather than the reverse[94]. In the combined analysis of multiplex imaging and spatial transcriptomics, it was also found that exhaustion hotspots are often located on the tumor side of the tumor-immune interface, co-occurring with suppressive axes[19]. Therefore, evaluating immune functionality requires more than just considering immune quantity or the presence of hotspots; it also necessitates assessing state score × hotspot position/type in tandem. CongMa et al. introduced CalicoST, providing a critical link to trace expression signals back to genetic drivers, thereby closing the loop of the spatial evidence to mechanism and decision cycle[94].

3. AI-driven Multiscale Data Integration and Virtual Cell Construction

Cells exist and interact in 3D space, and 3D tissue reconstruction enhances our understanding of disease mechanisms[8, 12, 24]. The key advantage of spatial omics is its spatial sensitivity—the ability to analyze molecular profiles of cells in their original tissue context. This makes it possible to capture critical features like immune infiltration, cell-cell interactions, and clonal organization, all of which serve as building blocks for creating computable virtual organs[95-97]. Complementary high-dimensional inputs, such as spectral cytometry data

profiling immune cell subsets, further refine the cellular representation, particularly for modeling the complex immune landscape relevant to cytotoxic therapies[98, 99].

Once spatial omics has mapped out the complexity of tumor ecology, the next challenge is turning that high dimensional, heterogeneous, and spatiotemporally scattered data into computable biological units. Solving this is key to moving spatial insights toward actual clinical use in diagnosis and treatment. Systematic differences across platforms in resolution, throughput, measurable molecular dimensions, and sampling intervals make information alignment and cross-validation more difficult[48, 95]. AI, particularly graph neural networks (GNNs), generative models, and Bayesian temporal models, offer new avenues for cross-modal integration and dynamic simulation, enabling spatial remodeling and providing a novel bridge for translating basic research into clinical practice[55, 100-103].

3.1 Unified Representation Specific to Tumors

Tumors may be regarded as a diverse cell system of different environments that provide information repeatedly, thereby stimulating change. A unified representation for tumor (UR-Tumor) has been introduced as a tumor-specific unified representation framework aimed at providing a coherent digital description at the cellular-microenvironment level[17, 104]. Virtual cells achieve an operable and sharable state by mapping biological data into the UR space. Spatial omics data, through the construction of cell activity, converts static spatial images into dynamic, updatable virtual cell bases, and both complement each other[95].

In the process of virtual cell modelling, an ideal approach is to build a model across three levels: molecular types, single cells, and multiple cells [105]. When modelling a single type of molecule, large language models may be more appropriate for dynamic modelling, although this method will lose information compared to atomic-level modelling approaches [106, 107]. When building the state of individual cells, molecular interactions and signal networks are used, and molecular or imaging-specific representations are employed to construct unit construction [108-110]. Swat et al. using CompuCell3D to develop a multi-cellular virtual tissue model. In this model, the external factors (such as nutrient and oxygen gradients, boundary conditions) were taken into account as limitations; while the internal inheritable physical parameters of the biological objects (for example, cell

adhesion force, survival threshold) were regarded as variables to be adjusted[111]. tably obtain the function expression of these units to ensure that the prediction results are accurate, and at the same time maintain mechanism interpretation ability and system scalability. For multi-cellular model building, there are more demands for space information. Spatial characteristics in two-dimensional tissue slices and three-dimensional tissue volumes, such as spatial signatures, can be obtained by simulating with graph learning techniques, for example, GNNs and equivariant neural networks[112-114]. Jeong et al. in their research on lung adenocarcinoma. Using this model to determine the exhaustion pattern of $CD8^+$ T cells at the tumor interface and successfully predict responses to immune checkpoint blockade.[115].

The main task of UR-Tumor is to achieve cross-modal alignment via multi-modal representation. In this research work, cross-modal alignment is realized through joint training of the three types of data for joint embedding space construction during the learning process: transcriptomics, proteomics and morphology. Contemporary multimodal deep frameworks build a shared latent Space. In spatial omics, methods such as Tangram and DestVI are particularly appropriate[102, 116]. For instance, combining spatial transcriptomics with multiplex immunofluorescence protein maps via a shared embedding reduces batch effects and inter-slice variations[117-119]. Uncertainty estimation is necessary; Bayesian neural networks or Monte Carlo dropout estimate uncertainty, and if it exceeds the threshold, reacquisition and re-evaluation can further overload the analytic pipeline[120, 121]. Spatial batch-effect alignment in spatial omics can use Harmony or Seurat variants, and spatial regularisation can be applied to maintain the geometric structure. Such cross-modal alignment also supports three-dimensional reconstruction to infer the tissue-level architecture from a limited number of sections[122-125].

The static model is unable to take into account the deformation under treatment; The multilevel virtual cell can cover time factors and achieve long-term information fusion using Bayesian filters or neural differential equation approaches. The newly obtained spatial omics data can be used to update the cellular state-transition matrix through particle filtering, thereby predicting the evolution of drug-resistant clones under multiple cycles of chemotherapy[126-128]. In principle, this framework is expected to include new spatial omics data after each treatment cycle, and UR-Tumor will be upgraded from a static substrate to a dynamic representation[129].

Combining various types of data from sequencing and imaging using AI to create a live-cell model for scientists. This tool can also display an animation and has some other features. It is possible to observe the change in expression of many genes at different stages and under various conditions for organisms at all life stages. This helps the researchers in their studies of the tumor environment across various scales.

3.2 Oncology-Specific Virtual Instrument

Multimodal foundation models across RNA, proteins, and DNA can be assembled into virtual cells, and further expanded to patient-specific VTOs [68, 130]. Based on UR-Tumor, virtual instrumentation for therapy (VI-Therapy) is proposed as a special kind of virtual instrument that operates on UR-Tumor embeddings to perform various functions and tasks at the patient level, such as simulation and decision-making support. By perturbing the URs of molecules, cells and tissues as input, the decoder is able to embed biological entities and predict one or more specific attributes, such as physical structure, cell type/state, adaptability, expression pattern, drug response[17].

Wenckstern et al. developed VirTues as a typical virtual tissue base model that can learn unified cross-scale representations of spatial proteomics data. Key design features include: protein language model embeddings for marker identity encoding, factorised attention mechanisms to process high-dimensional data, and hierarchical summary tokens that support multi-scale analysis. As shown in the triple-negative breast cancer case mentioned above, based on the virtual biomarkers we have derived from pre-treatment biopsy samples of patients, it can be predicted whether Anti-PD-L1 therapy will be effective for these patients; At the same time, combined with these data, we can also assess their survival status more accurately than through other methods. Models that can generate such high-quality tissue representations provide a technical support for VI-Therapy[131].

Virtual biopsy can be realised in VI-Therapy as the main function. Through the use of UR-Tumor to produce spatial risk maps that highlight high-risk areas, such as simulating sample collection along vascular paths in glioblastoma to predict drug infiltration and the dispersion patterns of stem-like tumor cells, without additional invasive procedures[132]. Sandy Figiel, et al., in prostate cancer. analysed gene expression of different prognostic features in a virtual biopsy framework to further investigate tumor heterogeneity [133]. This capability is based on the generative adversarial network or diffusion model to convert stochastic noise into structured output, that is, images or text, thereby imputing the unobserved region and ensuring the realism of simulation[134, 135]. Virtual

tumor models can be evaluated based on multi-feature integrative classifiers and performance indicators to improve virtual diagnosis and treatment plans[136, 137].

Therapeutic what-if simulations expand the scope of VI-Therapy, and local-to-systemic effects of dosing, sequencing, and combination regimens can be modelled. Ji GW and others. Devised an immune-ML model based on gradient boosting machines, showing that dense, reactive stroma restricts immune infiltration and, together with PD-1/PD-L1-mediated functional suppression, defines a high-risk group, thereby demonstrating an "immune infiltration gradient"[138]. In immunotherapy, such simulations can also be expanded to evaluate the reversal of interface-level exhaustion by PD-1 blockage and to simulate the dynamics of T-cell infiltration[139].

The prioritisation of combination strategies can be optimised using Monte Carlo Tree Search or reinforcement learning, thereby improving dose, the order of radio-, chemotherapy and immunotherapy, and their combined design - an implementable path to individualised cancer treatment[140-142].

By using AI to convert spatial omics data into a dynamic framework of virtual cells, we have taken an essential step toward the precise, scalable translation of basic research findings into clinical oncology applications. UR-Tumor provides a unified representation of cancer-related spatial omics, and VI-Therapy presents clinically oriented simulation; together, they support the Construction of VTE.

4. From VTCs to VTOs and Patient-Level Applications

Single static space data is difficult to directly serve as a medical tool for doctors in their work at the hospital. However, when scientists develop a tumor-specific VTE integrating AI technology that moves from virtual cells to VTOs, using multi-scale modelisation is feasible. In addition, by combining the information before and after treatment, a loop is formed that varies for each patient to ensure the effectiveness of therapy[143, 144]. Compared with the previous model, this one emphasises online updating and Uncertainty is handled more flexibly to maintain its practicability in the clinic. This way, the doctor can use the idea in a computer model, optimise the treatment plan according to his own situation and needs of each patient, as well as judge whether there is a tendency for drug resistance earlier.[145, 146].

4.1 VTE Assembling

The assembly of a VTE can be conceptualised as a multi-layered reconstruction process based on spatial data, which begins with the generation of virtual cells and continues to grow into a three-dimensional, multi-cellular, multi-clonal model capable of replicating the complex interactions within the TME. Throughout this progression, cellular spatial signatures, such as signaling mechanisms driven by cytokine gradients and receptor activation, molecular gradients shaped by the distribution of oxygen, nutrients, and metabolites, and interface dynamics arising from cell-cell interactions, serve as core components. These elements are realised by instantiating agents, cellular automata and so on[147, 148]. For example, in the agent-based model, the state-transition probability of agents is adjusted to imitate clonal expansion, immune evasion, and other processes[149].

To enhance the realism of VTE, the finite element method can be used in assembly to simulate diffusion fields and obtain permeability and uneven distributions under drug gradients[150]. The state switching, clonal expansion and immune escape of the other situation derived are respectively regulated in accordance with each other's states under different rules to achieve this conclusion[15, 151].

To ensure the robustness of the model in VTE assembly, uncertainty management is needed. By introducing Monte Carlo sampling or Bayesian inference at each simulation stage, the model can quantify parametric uncertainty; If this uncertainty exceeds the set threshold, it needs to be determined that parameters require readjustment or more data need to be collected[152]. This robustness makes VTE particularly applicable to highly complex tumors, such as glioblastoma[153]. VTE, combined with digital-twin ecosystems, can be expanded to a whole-body scale for modelling metastatic spread and systemic responses[151] (Figure 3).

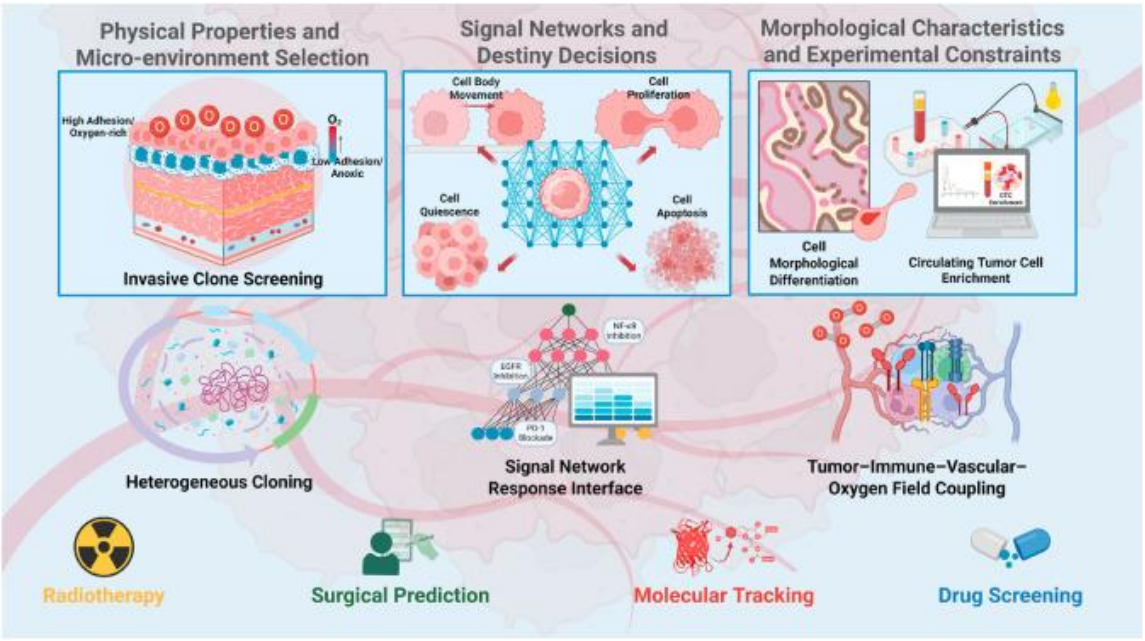

Fig. 3. Schematic diagram of the cross-scale role of VTCs towards patient level clinical use.

Reproduced with permission from Copyright 2025,[154] *Bioactive Materials*

4.2 Patient-Level Digital Update Pipeline

VTE Construction requires integrating data from multiple aspects, including electronic health records, Genomic Information and Imaging Examinations, Laboratory indicators; otherwise, it will not be possible to provide a solid foundation for its Digitalisation. In terms of clinical application, VTE needs to be embedded in a system-level digital update chain, and through a closed-loop feedback loop, it continuously optimises the pathway from signal acquisition to decision-making output. During acquisition, sparse sampling of the key molecular features and spatial compositional analysis are combined with AI-driven image-morphology registration for an initial VTE evaluation model. Here, scalable and robust spatial clustering algorithms are needed to quickly identify non-continuous tissue domains and micro-environmental niches from the sparse clinical inputs, ensuring timely model re-calibration[155]. Over time, new data will be introduced into the system. Use tools such as Kalman filters to promptly update the data from new observations in combination with the UR-Tumor model. Also uses area under the receiver operating characteristic curve and other indicators to monitor its own performance[151, 156]. To ensure that these updates are reflected in the evolution of living organisms rather than discrepancies among different operating conditions; To achieve high-quality connections between new sample data and previous

digital twins through excellent professional skills, scientists will improve this situation. At this point, it is necessary to eliminate batch effects while maintaining the genuine differences in biology[157].

To ensure that the modifications at different stages of time can reflect actual biological variations rather than differences in sample collection or processing, means must be found to achieve simultaneous updates of the new samples in the digital twin system. They need to eliminate batch effects while retaining the genuine differences in biology[158]. Scientists can add out-of-distribution detectors to the VTE while it is observing things. Many different models and training sets have been applied to these tools, which generally work effectively without any complications. Measure the uncertainty of the monitored stream. When confidence falls below a certain threshold, the system will recommend doing another biopsy or obtaining new imaging data[159]. People must still verify the work. The expert needs to ensure that the representation of tumors in the Digital Twin environment mirrors reality faithfully. They must carefully confirm that what the model is making up and predicting matches their own judgment and laboratory test data. Drug companies and research institutes have begun exploring the application of digital twins in the clinic. Building a complete digital twin for each patient is still the main objective of medicine in the future[151].

To apply this work more widely in clinical settings for use by doctors requires solving several key problems [160]. In terms of applying this in the clinic, the system needs to integrate with the way doctors work. It should only request new data or updates at times when doctors normally make decisions. Or it can be observed on its own, and an update will be triggered if there is any uncertainty; the limit of "uncertainty" is set according to the risk that the patient can tolerate. The model must also provide answers that doctors can apply in their work. Scientist need to actually test it in the natural environment to determine whether this prediction, such as the reduction of tumor size and extended survival free of cancer recurrence, can be achieved. Curve area and C-index would be used in tools. When the model presents information to the doctor, it should be displayed on a clear screen with useful graphics, such as maps of risk and side-by-side comparisons of different treatments, along with a list of options ranked by their potential effectiveness[161].

4.3 The Current State of Digital Twin Development

At the cellular level, researchers have integrated six omics modalities across cell lines and human tissue samples from ten types of tumors to build a database of protein and peptide targets involving multiple therapeutic

pathways, and conduct simulations of drug-cell interactions and the development of resistance[145, 162].At the tissue-organ level, there are virtual tumors such as Oncosimulator that integrate genomics, proteomics, metabolomics and imaging to recreate the space-time evolution at the supercellular and tissue levels. Wang and others. Calibrated data from mouse bladder cancer studies to build virtual tumors with high- and low-antigenicity tumor cells and different cytotoxic T lymphocyte killing mechanisms. By comparing agent-based models and ordinary differential equation models, it was found that the spatial complexity of the TME has a significant impact on the effect of PD-1/PD-L1 immune checkpoint inhibitors[163]. Within the European CHIC project, this platform has been used for preoperative chemotherapy of Wilms' tumor and radiotherapy response prediction of non-small cell lung cancer, and it has shown high consistency with actual clinical paths[144, 164]. At the patient level, the GLIOMATH study achieved a clinical validation of an individualised biomechanical model for glioblastoma, which utilises patient magnetic resonance imaging data to rebuild a biochemically and mechanically coupled virtual TME. The model reached 99 per cent consistency with the actual observation of tumor growth in one patient, a 55-year-old person, for eight months; Therefore, it has become the first to achieve tumor digital twin post-operation monitoring and treatment plan[165]. Analogous systems, CPDT and the DITTO visual digital twins, have also built individualised cancer-evolution models and interactive virtual-patient frameworks based on multimodal data for breast cancer and head-and-neck malignancies, respectively[166, 167].

Through various combinations of different types of data, VTE links fundamental biology with translational medicine. This will help promote the development of precision oncology. Cancer research is applying the concept of digital twins. To help scientists and doctors handle the complex situation and many difficulties in drug development in the laboratory and clinical trials. This provides a basis for making adjustments to treatments tailored to individuals in reality.

5. Limitations and Challenges

Despite the considerable clinical promise of combining spatial omics with VTOs, the field still faces substantial hurdles. First, cross-modal alignment and integration remain technically immature. Integrating spatial transcriptomic, proteomic, and epigenomic data into a unified representational format is prone to failure modes.

Although AI can assist with unification by leveraging large-scale data, both the construction of faithful virtual cell models and the realization of patient-updatable VTEs impose stringent demands on cross-modal data quality and analytic pipelines[168, 169]. In the near term, efforts to integrate data across institutions will likely face difficulties due to batch effects and interoperability issues caused by differing spatial omics platforms and protocols, further compromising model robustness and generalizability.

At the same time, current approaches for building virtual cells and organoids are still not fully developed. As an emerging field, initial progress has been made methodologically, but validation evidence and real-world use remain limited[170]. Progress is restricted due to the deficient amount of measured data and a lack of standardisation in model establishment.

Second, using deep learning in this way carries inherent methodological risks that need to be recognised [171]. One problem is that deep neural networks operate as Black Boxes. Therefore, doctors cannot understand the reasons for the conclusions reached. If the reason why the virtual models are established remains unknown to the doctors, they will not trust such models in their planning of significant treatments. The generative AI models that create virtual cells can also "hallucinate". Create some biological situations that may appear real but do not actually exist[172, 173]. As neural networks are not transparent, doctors are unable to understand the reasons behind their decisions. If the model remains hidden, clinicians will not be able to use it in clinical treatment for reference. Generative AI can also fabricate content. It generates biological details that appear realistic but are not actually present[161, 174].

In addition, spatial analysis based on biopsy samples is limited by the representativeness of the biopsy, and factors such as tissue subtypes, tumor grades, and clonal compositions may all influence expression patterns, thereby affecting the credibility of virtual-organ predictions[133]. Although spatial omics workflows are naturally integrated into routine histopathological processes and spatial omics technologies complement virtual cell construction, clinical translation still needs standardised procedures and validation frameworks[15]. Especially when these models are used to make decisions that need to be supported by them, the output should have transparency and can be verified. As the findings reported by Sandy Figiel et al., even though virtual tumor

biopsies reveal that there are considerable expression distinctions among different grade groups and tumor clones at the bulk level, such an analysis may still be incorrect in defining the gene signature[133].

In addition, there is a basic problem with the scale and complexity of the data: The amount of biological sequence data is enormous, but the capacity of mainstream AI training corpora is still limited. Systematic research on the scaling laws of model performance is required, as well as robust strategies for filtering and precisely discarding redundant data[175]. In addition, the construction and continuous updating of patient-specific digital twins require substantial computing power; large-scale spatial omics data processing and complex AI model training need significant graphics processing unit resources and scalable cloud infrastructure[171].

In addition to the technical difficulties and logistical troubles involved, there are severe problems with data privacy protection, project management, and ethical review in the application of patient data for constructing clinical models of VTE and virtual twins. How to leverage existing AI ethics frameworks and integrate them with medical regulation to build an ethical framework for patient digital models remains a pressing and unresolved issue[171, 176].

6. Outlook

As the foundation models that have achieved joint pre-training at the RNA, protein, and epigenetic levels continue to develop, it is possible that a leap from "virtual cells" to truly patient-specific "VTOs" would be realised. These systems could be used to carry out virtual biopsies at each treatment cycle, simulate and evaluate therapeutic regimens; Convert the spatial omics evidence in tumor cells into calibrated, continuously adjustable personalised clinical decisions. Finally, based on VTCs-based VTOs multi-institutional data sharing, standardised platforms, and cross-disciplinary cooperation, VTOs may become the core infrastructure of precision oncology, accelerating the digital transformation of cancer care[177]

7. Conclusion

Spatial omics technologies are changing people's understanding of tumor ecology by uncovering the molecular, cellular and spatial organisation of the TME. The data summarised above combined with VTEs will be transformed into practical precision oncology. Through the construction of UR-Tumor and VI-Therapy, dynamic

VTCs can be used as the computational foundation to simulate the development of tumors, predict drug responses, and develop personalised treatment plans.

Future research needs to focus on the standardisation of data integration pipelines, ensure the transparency of models, strengthen multi-institutional data sharing, and achieve clinically validated, continuously updatable digital twins. Finally, dynamic VTEs can address the disconnect between molecular evidence and clinical application in cancer treatment to drive its digitalisation process.

Abbreviations

TME: tumor microenvironment

STI: spatial-temporal-individualization

VTCs: virtual tumor cells

VTOs: virtual tumor organs

VTE: virtual tumor ecosystem

AI: artificial intelligence

MSI: mass spectrometry imaging

ECM: extracellular matrix

CAF: cancer-associated fibroblast

GNNs: graph neural networks

UR-Tumor: unified representation for tumor

VI-Therapy: virtual instrumentation for therapy

seqFISH (+): sequential fluorescence in situ hybridization (plus);

FFPE: formalin-fixed, paraffin-embedded;

FF: fresh frozen;

MERFISH: multiplexed error-robust fluorescence in situ hybridization;

STARmap: spatially resolved transcript amplicon readout mapping;

ExSeq: expansion sequencing;

IMC: imaging mass cytometry;

TME: tumor microenvironment;

MIBI-TOF: multiplexed ion beam imaging by time of flight;

LCM: laser capture microdissection;

WGBS: whole-genome bisulfite sequencing;

Geo-seq: geographical positioning sequencing;

ATAC: assay for transposase-accessible chromatin;

H&E: hematoxylin and eosin;

CNV: copy-number variation;

ATAC-seq: assay for transposase-accessible chromatin sequencing;

CUT&Tag: cleavage under targets and tagmentation;

sciMAP-ATAC: single-cell combinatorial indexing with spatial mapping

ATAC-seq; MSI: mass spectrometry imaging;

MALDI-MSI: matrix-assisted laser desorption/ionization mass spectrometry imaging;

DESI-MSI: desorption electrospray ionization mass spectrometry imaging;

ToF-SIMS: time-of-flight secondary ion mass spectrometry;

IHC: immunohistochemistry;

IF: immunofluorescence;

DBiT-seq: deterministic barcoding in tissue sequencing;

WTA: Whole Transcriptome Atlas;

ROI: Region Of Interest

EMT: epithelial-mesenchymal transition

Conflicts of Interest

The authors declare no conflicts of interest.

Funding

This research did not receive any specific grant from funding agencies in the public, commercial, or not-for-profit sectors.

Author contributions

Conceptualization: C.L., K.L.; Investigation and Formal analysis: K.L.; Visualization: K.L., R.Z.; Writing—original draft preparation: K.L.; Writing—review and editing: C.L., K.L., Y.L., G.H., R.Z.; Supervision: C.L. All authors have read and agreed to the published version of the manuscript.

Acknowledgments: None

AI-Disclosure: We thank GPT-5 (ChatGPT, OpenAI) for English language polishing. All authors reviewed, verified, and take full responsibility for the content and interpretations.

8. References

(1) Galon, J.; Bruni, D. Approaches to treat immune hot, altered and cold tumors with combination immunotherapies. *Nat Rev Drug Discov* **2019**, *18* (3), 197-218. DOI: https://doi.org/10.1038/s41573-018-0007-y.

(2) Janiszewska, M. The microcosmos of intratumor heterogeneity: the space-time of cancer evolution. *Oncogene* **2019**, *39* (10), 2031-2039. DOI: https://doi.org/10.1038/s41388-019-1127-5.

(3) Fan, J.; Slowikowski, K.; Zhang, F. Single-cell transcriptomics in cancer: computational challenges and opportunities. *Exp Mol Med* **2020**, *52* (9), 1452-1465. DOI: https://doi.org/10.1038/s12276-020-0422-0.

(4) McGranahan, N.; Swanton, C. Clonal Heterogeneity and Tumor Evolution: Past, Present, and the Future. *Cell* **2017**, *168* (4), 613-628. DOI: https://doi.org/10.1016/j.cell.2017.01.018.

(5) Mo, C.-K.; Liu, J.; Chen, S.; Storrs, E.; Targino da Costa, A. L. N.; Houston, A.; Wendl, M. C.; Jayasinghe, R. G.; Iglesia, M. D.; Ma, C.; et al. Tumor evolution and microenvironment interactions in 2D and 3D space. *Nature* **2024**, *634* (8036), 1178-1186. DOI: https://doi.org/10.1038/s41586-024-08087-4.

(6) Qu, Y.; Dou, B.; Tan, H.; Feng, Y.; Wang, N.; Wang, D. Tumor microenvironment-driven non-cell-autonomous resistance to antineoplastic treatment. *Mol Cancer* **2019**, *18* (1), 69. DOI: https://doi.org/10.1186/s12943-019-0992-4.

(7) Schott, M.; León-Periñán, D.; Splendiani, E.; Strenger, L.; Licha, J. R.; Pentimalli, T. M.; Schallenberg, S.; Alles, J.; Samut Tagliaferro, S.; Boltengagen, A.; et al. Open-ST: High-resolution spatial transcriptomics in 3D. *Cell* **2024**, *187* (15). DOI: https://doi.org/10.1016/j.cell.2024.05.055.

(8) Pentimalli, T. M.; Karaiskos, N.; Rajewsky, N. Challenges and Opportunities in the Clinical Translation of High-Resolution Spatial Transcriptomics. *Annu Rev Pathol* **2025**, *20* (1), 405-432. DOI: https://doi.org/10.1146/annurev-pathmechdis-111523-023417.

(9) Gulati, G. S.; D'Silva, J. P.; Liu, Y.; Wang, L.; Newman, A. M. Profiling cell identity and tissue architecture with single-cell and spatial transcriptomics. *Nat Rev Mol Cell Biol* **2025**, *26* (1), 11-31. DOI: https://doi.org/10.1038/s41580-024-00768-2.

(10) Lewis, S. M.; Asselin-Labat, M.-L.; Nguyen, Q.; Berthelet, J.; Tan, X.; Wimmer, V. C.; Merino, D.; Rogers, K. L.; Naik, S. H. Spatial omics and multiplexed imaging to explore cancer biology. *Nat Methods* **2021**, *18* (9), 997-1012. DOI: https://doi.org/10.1038/s41592-021-01203-6.

(11) Cervilla, S.; Grases, D.; Perez, E.; Real, F. X.; Musulen, E.; Aprea, J.; Esteller, M.; Porta-Pardo, E. Benchmarking of spatial transcriptomics platforms across six cancer types. *bioRxiv* **2025**, 2024.2005.2021.593407. DOI: 10.1101/2024.05.21.593407.

(12) Xu, X.; Su, J.; Zhu, R.; Li, K.; Zhao, X.; Fan, J.; Mao, F. From morphology to single-cell molecules: high-resolution 3D histology in biomedicine. *Mol Cancer* **2025**, *24* (1), 63. DOI: https://doi.org/10.1186/s12943-025-02240-x.

(13) Hui, T.; Zhou, J.; Yao, M.; Xie, Y.; Zeng, H. Advances in Spatial Omics Technologies. *Small Methods* **2025**, *9* (5), e2401171. DOI: https://doi.org/10.1002/smtd.202401171.

(14) Singhal, V.; Chou, N.; Lee, J.; Yue, Y.; Liu, J.; Chock, W. K.; Lin, L.; Chang, Y.-C.; Teo, E. M. L.; Aow, J.; et al. BANKSY unifies cell typing and tissue domain segmentation for scalable spatial omics data analysis. *Nat Genet* **2024**, *56* (3), 431-441. DOI: https://doi.org/10.1038/s41588-

024-01664-3.
(15) De Domenico, M.; Allegri, L.; Caldarelli, G.; d'Andrea, V.; Di Camillo, B.; Rocha, L. M.; Rozum, J.; Sbarbati, R.; Zambelli, F. Challenges and opportunities for digital twins in precision medicine from a complex systems perspective. *NPJ Digital Medicine* **2025**, *8* (1), 37. DOI: 10.1038/s41746-024-01402-3.
(16) Mollica, L.; Leli, C.; Sottotetti, F.; Quaglini, S.; Locati, L. D.; Marceglia, S. Digital twins: a new paradigm in oncology in the era of big data. *ESMO Real World Data and Digital Oncology* **2024**, *5*, 100056. DOI: https://doi.org/10.1016/j.esmorw.2024.100056.
(17) Bunne, C.; Roohani, Y.; Rosen, Y.; Gupta, A.; Zhang, X.; Roed, M.; Alexandrov, T.; AlQuraishi, M.; Brennan, P.; Burkhardt, D. B.; et al. How to build the virtual cell with artificial intelligence: Priorities and opportunities. *Cell* **2024**, *187* (25), 7045-7063. DOI: https://doi.org/10.1016/j.cell.2024.11.015.
(18) Williams, H. L.; Frei, A. L.; Koessler, T.; Berger, M. D.; Dawson, H.; Michielin, O.; Zlobec, I. The current landscape of spatial biomarkers for prediction of response to immune checkpoint inhibition. *npj Precision Oncology* **2024**, *8* (1), 178. DOI: https://doi.org/10.1038/s41698-024-00671-1.
(19) Keren, L.; Bosse, M.; Marquez, D.; Angoshtari, R.; Jain, S.; Varma, S.; Yang, S.-R.; Kurian, A.; Van Valen, D.; West, R.; et al. A Structured Tumor-Immune Microenvironment in Triple Negative Breast Cancer Revealed by Multiplexed Ion Beam Imaging. *Cell* **2018**, *174* (6), 1373-1387.e1319. DOI: https://doi.org/10.1016/j.cell.2018.08.039.
(20) Ciepła, J.; Smolarczyk, R. Tumor hypoxia unveiled: insights into microenvironment, detection tools and emerging therapies. *Clin Exp Med* **2024**, *24* (1), 235. DOI: https://doi.org/10.1007/s10238-024-01501-1.
(21) Shen, X.; Pan, D.; Gong, Q.; Gu, Z.; Luo, K. Enhancing drug penetration in solid tumors via nanomedicine: Evaluation models, strategies and perspectives. *Bioactive Materials* **2024**, *32*, 445-472. DOI: https://doi.org/10.1016/j.bioactmat.2023.10.017.
(22) Wang, H.; Arulraj, T.; Ippolito, A.; Popel, A. S. From virtual patients to digital twins in immuno-oncology: lessons learned from mechanistic quantitative systems pharmacology modeling. *NPJ Digit Med* **2024**, *7* (1), 189. DOI: https://doi.org/10.1038/s41746-024-01188-4.
(23) Eng, C.-H. L.; Lawson, M.; Zhu, Q.; Dries, R.; Koulena, N.; Takei, Y.; Yun, J.; Cronin, C.; Karp, C.; Yuan, G.-C.; et al. Transcriptome-scale super-resolved imaging in tissues by RNA seqFISH. *Nature* **2019**, *568* (7751), 235-239. DOI: https://doi.org/10.1038/s41586-019-1049-y.
(24) Cadinu, P.; Sivanathan, K. N.; Misra, A.; Xu, R. J.; Mangani, D.; Yang, E.; Rone, J. M.; Tooley, K.; Kye, Y.-C.; Bod, L.; et al. Charting the cellular biogeography in colitis reveals fibroblast trajectories and coordinated spatial remodeling. *Cell* **2024**, *187* (8). DOI: https://doi.org/10.1016/j.cell.2024.03.013.
(25) Marco Salas, S.; Kuemmerle, L. B.; Mattsson-Langseth, C.; Tismeyer, S.; Avenel, C.; Hu, T.; Rehman, H.; Grillo, M.; Czarnewski, P.; Helgadottir, S.; et al. Optimizing Xenium In Situ data utility by quality assessment and best-practice analysis workflows. *Nat Methods* **2025**, *22* (4), 813-823. DOI: https://doi.org/10.1038/s41592-025-02617-2.
(26) Liu, Y.; Dai, Y.; Wang, L. Spatial omics at the forefront: emerging technologies, analytical innovations, and clinical applications. *Cancer Cell* **2026**, *44* (1), 24-49. DOI: https://doi.org/10.1016/j.ccell.2025.12.009.
(27) Alon, S.; Goodwin, D. R.; Sinha, A.; Wassie, A. T.; Chen, F.; Daugharthy, E. R.; Bando, Y.; Kajita, A.; Xue, A. G.; Marrett, K.; et al. Expansion sequencing: Spatially precise in situ

transcriptomics in intact biological systems. *Science* **2021**, *371* (6528). DOI: https://doi.org/10.1126/science.aax2656.
(28) To, K.; Fei, L.; Pett, J. P.; Roberts, K.; Blain, R.; Polański, K.; Li, T.; Yayon, N.; He, P.; Xu, C.; et al. A multi-omic atlas of human embryonic skeletal development. *Nature* **2024**, *635* (8039), 657-667. DOI: https://doi.org/10.1038/s41586-024-08189-z.
(29) Shi, H.; He, Y.; Zhou, Y.; Huang, J.; Maher, K.; Wang, B.; Tang, Z.; Luo, S.; Tan, P.; Wu, M.; et al. Spatial atlas of the mouse central nervous system at molecular resolution. *Nature* **2023**, *622* (7983), 552-561. DOI: https://doi.org/10.1038/s41586-023-06569-5.
(30) Lee, J. H.; Daugharthy, E. R.; Scheiman, J.; Kalhor, R.; Yang, J. L.; Ferrante, T. C.; Terry, R.; Jeanty, S. S. F.; Li, C.; Amamoto, R.; et al. Highly multiplexed subcellular RNA sequencing in situ. *Science* **2014**, *343* (6177), 1360-1363. DOI: https://doi.org/10.1126/science.1250212.
(31) Zhao, Y.; Li, Y.; He, Y.; Wu, J.; Liu, Y.; Li, X.; Li, Z.; Yuan, Q.; Li, J.; Zhang, X.; et al. Stereo-seq V2: Spatial mapping of total RNA on FFPE sections with high resolution. *Cell* **2025**. DOI: https://doi.org/10.1016/j.cell.2025.08.008.
(32) Cable, D. M.; Murray, E.; Shanmugam, V.; Zhang, S.; Zou, L. S.; Diao, M.; Chen, H.; Macosko, E. Z.; Irizarry, R. A.; Chen, F. Cell type-specific inference of differential expression in spatial transcriptomics. *Nat Methods* **2022**, *19* (9), 1076-1087. DOI: https://doi.org/10.1038/s41592-022-01575-3.
(33) Russell, A. J. C.; Weir, J. A.; Nadaf, N. M.; Shabet, M.; Kumar, V.; Kambhampati, S.; Raichur, R.; Marrero, G. J.; Liu, S.; Balderrama, K. S.; et al. Slide-tags enables single-nucleus barcoding for multimodal spatial genomics. *Nature* **2023**, *625* (7993), 101-109. DOI: https://doi.org/10.1038/s41586-023-06837-4.
(34) Zhu, M.; Li, N.; Fan, L.; Wu, R.; Cao, L.; Ren, Y.; Lu, C.; Zhang, L.; Cai, Y.; Shi, Y.; et al. Single-cell transcriptomic and spatial analysis reveal the immunosuppressive microenvironment in relapsed/refractory angioimmunoblastic T-cell lymphoma. *Blood Cancer J* **2024**, *14* (1), 218. DOI: https://doi.org/10.1038/s41408-024-01199-0.
(35) McCaffrey, E. F.; Donato, M.; Keren, L.; Chen, Z.; Delmastro, A.; Fitzpatrick, M. B.; Gupta, S.; Greenwald, N. F.; Baranski, A.; Graf, W.; et al. The immunoregulatory landscape of human tuberculosis granulomas. *Nat Immunol* **2022**, *23* (2), 318-329. DOI: https://doi.org/10.1038/s41590-021-01121-x.
(36) Monasterio, G.; Morales, R. A.; Bejarano, D. A.; Abalo, X. M.; Fransson, J.; Larsson, L.; Schlitzer, A.; Lundeberg, J.; Das, S.; Villablanca, E. J. A versatile tissue-rolling technique for spatial-omics analyses of the entire murine gastrointestinal tract. *Nat Protoc* **2024**, *19* (10), 3085-3137. DOI: https://doi.org/10.1038/s41596-024-01001-2.
(37) Millian, D. E.; Saldarriaga, O. A.; Wanninger, T.; Burks, J. K.; Rafati, Y. N.; Gosnell, J.; Stevenson, H. L. Cutting-Edge Platforms for Analysis of Immune Cells in the Hepatic Microenvironment-Focus on Tumor-Associated Macrophages in Hepatocellular Carcinoma. *Cancers (Basel)* **2022**, *14* (8). DOI: https://doi.org/10.3390/cancers14081861.
(38) Zhao, T.; Chiang, Z. D.; Morriss, J. W.; LaFave, L. M.; Murray, E. M.; Del Priore, I.; Meli, K.; Lareau, C. A.; Nadaf, N. M.; Li, J.; et al. Spatial genomics enables multi-modal study of clonal heterogeneity in tissues. *Nature* **2021**, *601* (7891), 85-91. DOI: https://doi.org/10.1038/s41586-021-04217-4.
(39) Zhao, L.; Wu, X.; Zheng, J.; Dong, D. DNA methylome profiling of circulating tumor cells in lung cancer at single base-pair resolution. *Oncogene* **2021**, *40* (10), 1884-1895. DOI: https://doi.org/10.1038/s41388-021-01657-0.

(40) Tang, L. P.; Zhai, L. M.; Li, J.; Gao, Y.; Ma, Q. L.; Li, R.; Liu, Q. F.; Zhang, W. J.; Yao, W. J.; Mu, B.; et al. Time-resolved reprogramming of single somatic cells into totipotent states during plant regeneration. *Cell* **2025**. DOI: https://doi.org/10.1016/j.cell.2025.08.031.
(41) Thornton, C. A.; Mulqueen, R. M.; Torkenczy, K. A.; Nishida, A.; Lowenstein, E. G.; Fields, A. J.; Steemers, F. J.; Zhang, W.; McConnell, H. L.; Woltjer, R. L.; et al. Spatially mapped single-cell chromatin accessibility. *Nature Communications* **2021**, *12* (1), 1274. DOI: https://doi.org/10.1038/s41467-021-21515-7.
(42) Deng, Y.; Bartosovic, M.; Kukanja, P.; Zhang, D.; Liu, Y.; Su, G.; Enninful, A.; Bai, Z.; Castelo-Branco, G.; Fan, R. Spatial-CUT&Tag: Spatially resolved chromatin modification profiling at the cellular level. *Science* **2022**, *375* (6581), 681-686. DOI: https://doi.org/10.1126/science.abg7216.
(43) Deng, Y.; Bartosovic, M.; Ma, S.; Zhang, D.; Kukanja, P.; Xiao, Y.; Su, G.; Liu, Y.; Qin, X.; Rosoklija, G. B.; et al. Spatial profiling of chromatin accessibility in mouse and human tissues. *Nature* **2022**, *609* (7926), 375-383. DOI: https://doi.org/10.1038/s41586-022-05094-1.
(44) Planque, M.; Igelmann, S.; Ferreira Campos, A. M.; Fendt, S.-M. Spatial metabolomics principles and application to cancer research. *Curr Opin Chem Biol* **2023**, *76*, 102362. DOI: https://doi.org/10.1016/j.cbpa.2023.102362.
(45) Kumar, B. S. Desorption electrospray ionization mass spectrometry imaging (DESI-MSI) in disease diagnosis: an overview. *Anal Methods* **2023**, *15* (31), 3768-3784. DOI: https://doi.org/10.1039/d3ay00867c.
(46) Yoon, S.; Lee, T. G. Biological tissue sample preparation for time-of-flight secondary ion mass spectrometry (ToF-SIMS) imaging. *Nano Converg* **2018**, *5* (1), 24. DOI: https://doi.org/10.1186/s40580-018-0157-y.
(47) Cheng, Y.; Burrack, R. K.; Li, Q. Spatially Resolved and Highly Multiplexed Protein and RNA In Situ Detection by Combining CODEX With RNAscope In Situ Hybridization. *J Histochem Cytochem* **2022**, *70* (8), 571-581. DOI: https://doi.org/10.1369/00221554221114174.
(48) Marconato, L.; Palla, G.; Yamauchi, K. A.; Virshup, I.; Heidari, E.; Treis, T.; Vierdag, W.-M.; Toth, M.; Stockhaus, S.; Shrestha, R. B.; et al. SpatialData: an open and universal data framework for spatial omics. *Nat Methods* **2024**, *22* (1), 58-62. DOI: https://doi.org/10.1038/s41592-024-02212-x.
(49) Vicari, M.; Mirzazadeh, R.; Nilsson, A.; Shariatgorji, R.; Bjärterot, P.; Larsson, L.; Lee, H.; Nilsson, M.; Foyer, J.; Ekvall, M.; et al. Spatial multimodal analysis of transcriptomes and metabolomes in tissues. *Nature Biotechnology* **2023**, *42* (7), 1046-1050. DOI: https://doi.org/10.1038/s41587-023-01937-y.
(50) Liu, Y.; Yang, M.; Deng, Y.; Su, G.; Enninful, A.; Guo, C. C.; Tebaldi, T.; Zhang, D.; Kim, D.; Bai, Z.; et al. High-Spatial-Resolution Multi-Omics Sequencing via Deterministic Barcoding in Tissue. *Cell* **2020**, *183* (6). DOI: https://doi.org/10.1016/j.cell.2020.10.026.
(51) Galeano Niño, J. L.; Wu, H.; LaCourse, K. D.; Kempchinsky, A. G.; Baryiames, A.; Barber, B.; Futran, N.; Houlton, J.; Sather, C.; Sicinska, E.; et al. Effect of the intratumoral microbiota on spatial and cellular heterogeneity in cancer. *Nature* **2022**, *611* (7937), 810-817. DOI: https://doi.org/10.1038/s41586-022-05435-0.
(52) Rao, A.; Barkley, D.; França, G. S.; Yanai, I. Exploring tissue architecture using spatial transcriptomics. *Nature* **2021**, *596* (7871), 211-220. DOI: https://doi.org/10.1038/s41586-021-03634-9.
(53) Gyllborg, D.; Langseth, C. M.; Qian, X.; Choi, E.; Salas, S. M.; Hilscher, M. M.; Lein, E. S.; Nilsson, M. Hybridization-based in situ sequencing (HybISS) for spatially resolved

transcriptomics in human and mouse brain tissue. *Nucleic Acids Res* **2020**, *48* (19), e112. DOI: https://doi.org/10.1093/nar/gkaa792.
(54) Samuel, G. R.; Robert, R. S.; Aleksandrina, G.; Carly, A. M.; Evan, M.; Charles, R. V.; Joshua, W.; Linlin, M. C.; Fei, C.; Evan, Z. M. Slide-seq: A scalable technology for measuring genome-wide expression at high spatial resolution. *Science* **2019**, *363* (6434), 1463-1467. DOI: https://doi.org/10.1126/science.aaw1219.
(55) Zhang, Z.; Sun, Y.; Peng, Q.; Li, T.; Zhou, P. Integrating Dynamical Systems Modeling with Spatiotemporal scRNA-Seq Data Analysis. *Entropy (Basel)* **2025**, *27* (5). DOI: https://doi.org/10.3390/e27050453.
(56) Zhang, J.; Hou, L.; Ma, L.; Cai, Z.; Ye, S.; Liu, Y.; Ji, P.; Zuo, Z.; Zhao, F. Real-time and programmable transcriptome sequencing with PROFIT-seq. *Nat Cell Biol* **2024**, *26* (12), 2183-2194. DOI: https://doi.org/10.1038/s41556-024-01537-1.
(57) Kip, A. M.; Valverde, J. M.; Altelaar, M.; Heeren, R. M. A.; Hundscheid, I. H. R.; Dejong, C. H. C.; Olde Damink, S. W. M.; Balluff, B.; Lenaerts, K. Combined Quantitative (Phospho)proteomics and Mass Spectrometry Imaging Reveal Temporal and Spatial Protein Changes in Human Intestinal Ischemia-Reperfusion. *J Proteome Res* **2022**, *21* (1), 49-66. DOI: https://doi.org/10.1021/acs.jproteome.1c00447.
(58) Goltsev, Y.; Samusik, N.; Kennedy-Darling, J.; Bhate, S.; Hale, M.; Vazquez, G.; Black, S.; Nolan, G. P. Deep Profiling of Mouse Splenic Architecture with CODEX Multiplexed Imaging. *Cell* **2018**, *174* (4). DOI: https://doi.org/10.1016/j.cell.2018.07.010.
(59) Xu, Z.; Wang, Y.; Xie, T.; Luo, R.; Ni, H.-L.; Xiang, H.; Tang, S.; Tan, S.; Fang, R.; Ran, P.; et al. Panoramic spatial enhanced resolution proteomics (PSERP) reveals tumor architecture and heterogeneity in gliomas. *J Hematol Oncol* **2025**, *18* (1), 58. DOI: https://doi.org/10.1186/s13045-025-01710-5.
(60) Bressan, D.; Battistoni, G.; Hannon, G. J. The dawn of spatial omics. *Science* **2023**, *381* (6657), eabq4964. DOI: https://doi.org/10.1126/science.abq4964.
(61) Zhang, D.; Deng, Y.; Kukanja, P.; Agirre, E.; Bartosovic, M.; Dong, M.; Ma, C.; Ma, S.; Su, G.; Bao, S.; et al. Spatial epigenome–transcriptome co-profiling of mammalian tissues. *Nature* **2023**, *616* (7955), 113-122. DOI: https://doi.org/10.1038/s41586-023-05795-1.
(62) Zhang, H.; Lu, K. H.; Ebbini, M.; Huang, P.; Lu, H.; Li, L. Mass spectrometry imaging for spatially resolved multi-omics molecular mapping. *npj Imaging* **2024**, *2* (1), 20. DOI: https://doi.org/10.1038/s44303-024-00025-3.
(63) Spangenberg, P.; Bessler, S.; Widera, L.; Bottek, J.; Richter, M.; Thiebes, S.; Siemes, D.; Krauß, S. D.; Migas, L. G.; Kasarla, S. S.; et al. msiFlow: automated workflows for reproducible and scalable multimodal mass spectrometry imaging and microscopy data analysis. *Nature Communications* **2025**, *16* (1), 1065. DOI: https://doi.org/10.1038/s41467-024-55306-7.
(64) Spraggins, J. M.; Djambazova, K. V.; Rivera, E. S.; Migas, L. G.; Neumann, E. K.; Fuetterer, A.; Suetering, J.; Goedecke, N.; Ly, A.; Van de Plas, R.; et al. High-Performance Molecular Imaging with MALDI Trapped Ion-Mobility Time-of-Flight (timsTOF) Mass Spectrometry. *Analytical Chemistry* **2019**, *91* (22), 14552-14560. DOI: https://doi.org/10.1021/acs.analchem.9b03612.
(65) Rappez, L.; Stadler, M.; Triana, S.; Gathungu, R. M.; Ovchinnikova, K.; Phapale, P.; Heikenwalder, M.; Alexandrov, T. SpaceM reveals metabolic states of single cells. *Nat Methods* **2021**, *18* (7), 799-805. DOI: https://doi.org/10.1038/s41592-021-01198-0.
(66) Li, B.; Bao, F.; Hou, Y.; Li, F.; Li, H.; Deng, Y.; Dai, Q. Tissue characterization at an enhanced resolution across spatial omics platforms with deep generative model. *Nature Communications*

2024, *15* (1), 6541. DOI: https://doi.org/10.1038/s41467-024-50837-5.
(67) Coleman, K.; Schroeder, A.; Loth, M.; Zhang, D.; Park, J. H.; Sung, J.-Y.; Blank, N.; Cowan, A. J.; Qian, X.; Chen, J.; et al. Resolving tissue complexity by multimodal spatial omics modeling with MISO. *Nat Methods* **2025**, *22* (3), 530-538. DOI: https://doi.org/10.1038/s41592-024-02574-2.
(68) Cui, H.; Tejada-Lapuerta, A.; Brbić, M.; Saez-Rodriguez, J.; Cristea, S.; Goodarzi, H.; Lotfollahi, M.; Theis, F. J.; Wang, B. Towards multimodal foundation models in molecular cell biology. *Nature* **2025**, *640* (8059), 623-633. DOI: https://doi.org/10.1038/s41586-025-08710-y.
(69) Vandereyken, K.; Sifrim, A.; Thienpont, B.; Voet, T. Methods and applications for single-cell and spatial multi-omics. *Nat Rev Genet* **2023**, *24* (8), 494-515. DOI: https://doi.org/10.1038/s41576-023-00580-2.
(70) Kueckelhaus, J.; Frerich, S.; Kada-Benotmane, J.; Koupourtidou, C.; Ninkovic, J.; Dichgans, M.; Beck, J.; Schnell, O.; Heiland, D. H. Inferring histology-associated gene expression gradients in spatial transcriptomic studies. *Nature Communications* **2024**, *15* (1), 7280. DOI: https://doi.org/10.1038/s41467-024-50904-x.
(71) Berglund, E.; Maaskola, J.; Schultz, N.; Friedrich, S.; Marklund, M.; Bergenstråhle, J.; Tarish, F.; Tanoglidi, A.; Vickovic, S.; Larsson, L.; et al. Spatial maps of prostate cancer transcriptomes reveal an unexplored landscape of heterogeneity. *Nature Communications* **2018**, *9* (1), 2419. DOI: https://doi.org/10.1038/s41467-018-04724-5.
(72) Greenwald, A. C.; Darnell, N. G.; Hoefflin, R.; Simkin, D.; Mount, C. W.; Gonzalez Castro, L. N.; Harnik, Y.; Dumont, S.; Hirsch, D.; Nomura, M.; et al. Integrative spatial analysis reveals a multi-layered organization of glioblastoma. *Cell* **2024**, *187* (10). DOI: https://doi.org/10.1016/j.cell.2024.03.029.
(73) Landon-Brace, N.; Latour, S.; Innes, B. T.; Nurse, M.; Cadavid, J. L.; Co, I. L.; Tan, C. M.; Nowlan, F.; Drissler, S.; Notta, F.; et al. Analysis of an engineered organoid model of pancreatic cancer identifies hypoxia as a contributing factor in determining transcriptional subtypes. *Sci Rep* **2025**, *15* (1), 23610. DOI: https://doi.org/10.1038/s41598-025-98344-x.
(74) Terrassoux, L.; Hazard, C.; Laratte, A.; Balsamelli, J.; Arcicasa, M.; Fong, E.; Baland, L.; Soncin, F.; Cappello, G.; Maurage, C.-A.; et al. Novel Diffuse Midline Glioma-on-Chip Recapitulating Tumor Biophysical Microenvironment to Assess the Heterogeneity of Response to Therapies. *Small* **2025**, e05343. DOI: https://doi.org/10.1002/smll.202505343.
(75) Auxillos, J.; Crouigneau, R.; Li, Y.-F.; Dai, Y.; Stigliani, A.; Tavernaro, I.; Resch-Genger, U.; Sandelin, A.; Marie, R.; Pedersen, S. F. Spatially resolved analysis of microenvironmental gradient impact on cancer cell phenotypes. *Sci Adv* **2024**, *10* (18), eadn3448. DOI: https://doi.org/10.1126/sciadv.adn3448.
(76) Duncan, K. D.; Pětrošová, H.; Lum, J. J.; Goodlett, D. R. Mass spectrometry imaging methods for visualizing tumor heterogeneity. *Curr Opin Biotechnol* **2024**, *86*, 103068. DOI: https://doi.org/10.1016/j.copbio.2024.103068.
(77) Folz, J.; Jo, J.; Eido, A.; Gonzalez, M. E.; Caruso, R.; Kleer, C. G.; Wang, X. Photoacoustic Chemical Imaging of Tumor Microenvironment pH for Prediction of Chemotherapeutic Efficacy in Breast Cancer. *Nano Letters* **2025**. DOI: https://doi.org/10.1021/acs.nanolett.5c02756.
(78) Jove, M.; Spencer, J.; Clench, M.; Loadman, P. M.; Twelves, C. Precision pharmacology: Mass spectrometry imaging and pharmacokinetic drug resistance. *Critical Reviews in Oncology/Hematology* **2019**, *141*, 153-162. DOI: https://doi.org/10.1016/j.critrevonc.2019.06.008.

(79) Schürch, C. M.; Bhate, S. S.; Barlow, G. L.; Phillips, D. J.; Noti, L.; Zlobec, I.; Chu, P.; Black, S.; Demeter, J.; McIlwain, D. R.; et al. Coordinated Cellular Neighborhoods Orchestrate Antitumoral Immunity at the Colorectal Cancer Invasive Front. *Cell* **2020**, *182* (5). DOI: https://doi.org/10.1016/j.cell.2020.07.005.
(80) Dakal, T. C.; George, N.; Xu, C.; Suravajhala, P.; Kumar, A. Predictive and Prognostic Relevance of Tumor-Infiltrating Immune Cells: Tailoring Personalized Treatments against Different Cancer Types. *Cancers (Basel)* **2024**, *16* (9). DOI: https://doi.org/10.3390/cancers16091626.
(81) Allam, M.; Hu, T.; Lee, J.; Aldrich, J.; Badve, S. S.; Gökmen-Polar, Y.; Bhave, M.; Ramalingam, S. S.; Schneider, F.; Coskun, A. F. Spatially variant immune infiltration scoring in human cancer tissues. *NPJ Precision Oncology* **2022**, *6* (1), 60. DOI: https://doi.org/10.1038/s41698-022-00305-4.
(82) Griffin, G. K.; Weirather, J. L.; Roemer, M. G. M.; Lipschitz, M.; Kelley, A.; Chen, P.-H.; Gusenleitner, D.; Jeter, E.; Pak, C.; Gjini, E.; et al. Spatial signatures identify immune escape via PD-1 as a defining feature of T-cell/histiocyte-rich large B-cell lymphoma. *Blood* **2021**, *137* (10), 1353-1364. DOI: https://doi.org/10.1182/blood.2020006464.
(83) Wu, S. Z.; Al-Eryani, G.; Roden, D. L.; Junankar, S.; Harvey, K.; Andersson, A.; Thennavan, A.; Wang, C.; Torpy, J. R.; Bartonicek, N.; et al. A single-cell and spatially resolved atlas of human breast cancers. *Nat Genet* **2021**, *53* (9), 1334-1347. DOI: https://doi.org/10.1038/s41588-021-00911-1.
(84) Zhang, H.; AbdulJabbar, K.; Moore, D. A.; Akarca, A.; Enfield, K. S. S.; Jamal-Hanjani, M.; Raza, S. E. A.; Veeriah, S.; Salgado, R.; McGranahan, N.; et al. Spatial Positioning of Immune Hotspots Reflects the Interplay between B and T Cells in Lung Squamous Cell Carcinoma. *Cancer Res* **2023**, *83* (9), 1410-1425. DOI: https://doi.org/10.1158/0008-5472.Can-22-2589.
(85) Singhal, V.; Chou, N. BANKSY: scalable cell typing and domain segmentation for spatial omics. *Nat Rev Genet* **2024**, *25* (8), 527-528. DOI: https://doi.org/10.1038/s41576-024-00743-9.
(86) Danenberg, E.; Bardwell, H.; Zanotelli, V. R. T.; Provenzano, E.; Chin, S.-F.; Rueda, O. M.; Green, A.; Rakha, E.; Aparicio, S.; Ellis, I. O.; et al. Breast tumor microenvironment structures are associated with genomic features and clinical outcome. *Nat Genet* **2022**, *54* (5), 660-669. DOI: https://doi.org/10.1038/s41588-022-01041-y.
(87) Ali, H. R.; Jackson, H. W.; Zanotelli, V. R. T.; Danenberg, E.; Fischer, J. R.; Bardwell, H.; Provenzano, E.; Rueda, O. M.; Chin, S.-F.; Aparicio, S.; et al. Imaging mass cytometry and multiplatform genomics define the phenogenomic landscape of breast cancer. *Nat Cancer* **2020**, *1* (2), 163-175. DOI: https://doi.org/10.1038/s43018-020-0026-6.
(88) Feng, Y.; Ma, W.; Zang, Y.; Guo, Y.; Li, Y.; Zhang, Y.; Dong, X.; Liu, Y.; Zhan, X.; Pan, Z.; et al. Spatially organized tumor-stroma boundary determines the efficacy of immunotherapy in colorectal cancer patients. *Nature Communications* **2024**, *15* (1), 10259. DOI: https://doi.org/10.1038/s41467-024-54710-3.
(89) Ji, A. L.; Rubin, A. J.; Thrane, K.; Jiang, S.; Reynolds, D. L.; Meyers, R. M.; Guo, M. G.; George, B. M.; Mollbrink, A.; Bergenstråhle, J.; et al. Multimodal Analysis of Composition and Spatial Architecture in Human Squamous Cell Carcinoma. *Cell* **2020**, *182* (2). DOI: https://doi.org/10.1016/j.cell.2020.05.039.
(90) Yerly, L.; Pich-Bavastro, C.; Di Domizio, J.; Wyss, T.; Tissot-Renaud, S.; Cangkrama, M.; Gilliet, M.; Werner, S.; Kuonen, F. Integrated multi-omics reveals cellular and molecular

interactions governing the invasive niche of basal cell carcinoma. *Nature Communications* **2022**, *13* (1), 4897. DOI: https://doi.org/10.1038/s41467-022-32670-w.
(91) Cords, L.; Engler, S.; Haberecker, M.; Rüschoff, J. H.; Moch, H.; de Souza, N.; Bodenmiller, B. Cancer-associated fibroblast phenotypes are associated with patient outcome in non-small cell lung cancer. *Cancer Cell* **2024**, *42* (3). DOI: https://doi.org/10.1016/j.ccell.2023.12.021.
(92) Valdeolivas, A.; Amberg, B.; Giroud, N.; Richardson, M.; Gálvez, E. J. C.; Badillo, S.; Julien-Laferrière, A.; Túrós, D.; Voith von Voithenberg, L.; Wells, I.; et al. Profiling the heterogeneity of colorectal cancer consensus molecular subtypes using spatial transcriptomics. *NPJ Precision Oncology* **2024**, *8* (1), 10. DOI: https://doi.org/10.1038/s41698-023-00488-4.
(93) Jiang, R.; Li, Z.; Jia, Y.; Li, S.; Chen, S. SINFONIA: Scalable Identification of Spatially Variable Genes for Deciphering Spatial Domains. *Cells* **2023**, *12* (4). DOI: https://doi.org/10.3390/cells12040604.
(94) Ma, C.; Balaban, M.; Liu, J.; Chen, S.; Wilson, M. J.; Sun, C. H.; Ding, L.; Raphael, B. J. Inferring allele-specific copy number aberrations and tumor phylogeography from spatially resolved transcriptomics. *Nat Methods* **2024**, *21* (12), 2239-2247. DOI: https://doi.org/10.1038/s41592-024-02438-9.
(95) Du, J.; Yang, Y. C.; An, Z. J.; Zhang, M. H.; Fu, X. H.; Huang, Z. F.; Yuan, Y.; Hou, J. Advances in spatial transcriptomics and related data analysis strategies. *J Transl Med* **2023**, *21* (1), 330. DOI: https://doi.org/10.1186/s12967-023-04150-2.
(96) Jing, S.-Y.; Wang, H.-Q.; Lin, P.; Yuan, J.; Tang, Z.-X.; Li, H. Quantifying and interpreting biologically meaningful spatial signatures within tumor microenvironments. *NPJ Precision Oncology* **2025**, *9* (1), 68. DOI: https://doi.org/10.1038/s41698-025-00857-1.
(97) Lee, R. Y.; Ng, C. W.; Rajapakse, M. P.; Ang, N.; Yeong, J. P. S.; Lau, M. C. The promise and challenge of spatial omics in dissecting tumor microenvironment and the role of AI. *Front Oncol* **2023**, *13*, 1172314. DOI: https://doi.org/10.3389/fonc.2023.1172314.
(98) Gupta, P.; Dang, M.; Oberai, S.; Migliozzi, S.; Trivedi, R.; Kumar, G.; Peshoff, M.; Milam, N.; Ahmed, A.; Bojja, K.; et al. Immune landscape of isocitrate dehydrogenase-stratified primary and recurrent human gliomas. *Neuro Oncol* **2024**, *26* (12), 2239-2255. DOI: https://doi.org/10.1093/neuonc/noae139.
(99) Cordes, M.; Pike-Overzet, K.; Van Den Akker, E. B.; Staal, F. J. T.; Canté-Barrett, K. Multi-omic analyses in immune cell development with lessons learned from T cell development. *Front Cell Dev Biol* **2023**, *11*, 1163529. DOI: https://doi.org/10.3389/fcell.2023.1163529.
(100) Hu, J.; Li, X.; Coleman, K.; Schroeder, A.; Ma, N.; Irwin, D. J.; Lee, E. B.; Shinohara, R. T.; Li, M. SpaGCN: Integrating gene expression, spatial location and histology to identify spatial domains and spatially variable genes by graph convolutional network. *Nat Methods* **2021**, *18* (11), 1342-1351. DOI: https://doi.org/10.1038/s41592-021-01255-8.
(101) Long, Y.; Ang, K. S.; Li, M.; Chong, K. L. K.; Sethi, R.; Zhong, C.; Xu, H.; Ong, Z.; Sachaphibulkij, K.; Chen, A.; et al. Spatially informed clustering, integration, and deconvolution of spatial transcriptomics with GraphST. *Nature Communications* **2023**, *14* (1), 1155. DOI: https://doi.org/10.1038/s41467-023-36796-3.
(102) Lopez, R.; Li, B.; Keren-Shaul, H.; Boyeau, P.; Kedmi, M.; Pilzer, D.; Jelinski, A.; Yofe, I.; David, E.; Wagner, A.; et al. DestVI identifies continuums of cell types in spatial transcriptomics data. *Nat Biotechnol* **2022**, *40* (9), 1360-1369. DOI: https://doi.org/10.1038/s41587-022-01272-8.
(103) Sha, Y.; Qiu, Y.; Zhou, P.; Nie, Q. Reconstructing growth and dynamic trajectories from

single-cell transcriptomics data. *Nature Machine Intelligence* **2024**, *6* (1), 25-39. DOI: https://doi.org/10.1038/s42256-023-00763-w.
(104) Jafari Nivlouei, S.; Soltani, M.; Shirani, E.; Salimpour, M. R.; Travasso, R.; Carvalho, J. A multiscale cell-based model of tumor growth for chemotherapy assessment and tumor-targeted therapy through a 3D computational approach. *Cell Prolif* **2022**, *55* (3), e13187. DOI: https://doi.org/10.1111/cpr.13187.
(105) Metzcar, J.; Wang, Y.; Heiland, R.; Macklin, P. A Review of Cell-Based Computational Modeling in Cancer Biology. *JCO Clin Cancer Inform* **2019**, *3*. DOI: https://doi.org/10.1200/CCI.18.00069.
(106) Peng, F. Z.; Wang, C.; Chen, T.; Schussheim, B.; Vincoff, S.; Chatterjee, P. PTM-Mamba: a PTM-aware protein language model with bidirectional gated Mamba blocks. *Nat Methods* **2025**, *22* (5), 945-949. DOI: https://doi.org/10.1038/s41592-025-02656-9.
(107) Dai, B.; Mattox, D. E.; Bailey-Kellogg, C. Attention please: modeling global and local context in glycan structure-function relationships. *bioRxiv* **2021**, 2021.2010.2015.464532. DOI: https://doi.org/10.1101/2021.10.15.464532.
(108) Saar, K. L.; Scrutton, R. M.; Bloznelyte, K.; Morgunov, A. S.; Good, L. L.; Lee, A. A.; Teichmann, S. A.; Knowles, T. P. J. Protein Condensate Atlas from predictive models of heteromolecular condensate composition. *Nature Communications* **2024**, *15* (1), 5418. DOI: https://doi.org/10.1038/s41467-024-48496-7.
(109) Theodoris, C. V.; Xiao, L.; Chopra, A.; Chaffin, M. D.; Al Sayed, Z. R.; Hill, M. C.; Mantineo, H.; Brydon, E. M.; Zeng, Z.; Liu, X. S.; et al. Transfer learning enables predictions in network biology. *Nature* **2023**, *618* (7965), 616-624. DOI: https://doi.org/10.1038/s41586-023-06139-9.
(110) Kha, Q.-H.; Ho, Q.-T.; Le, N. Q. K. Identifying SNARE Proteins Using an Alignment-Free Method Based on Multiscan Convolutional Neural Network and PSSM Profiles. *J Chem Inf Model* **2022**, *62* (19), 4820-4826. DOI: https://doi.org/10.1021/acs.jcim.2c01034.
(111) Swat, M. H.; Thomas, G. L.; Shirinifard, A.; Clendenon, S. G.; Glazier, J. A. Emergent Stratification in Solid Tumors Selects for Reduced Cohesion of Tumor Cells: A Multi-Cell, Virtual-Tissue Model of Tumor Evolution Using CompuCell3D. *PLOS ONE* **2015**, *10* (6), e0127972. DOI: https://doi.org/10.1371/journal.pone.0127972.
(112) Zhu, H.; Ma, M.; Ma, W.; Jiao, L.; Hong, S.; Shen, J.; Hou, B. A spatial-channel progressive fusion ResNet for remote sensing classification. *Information Fusion* **2021**, *70*, 72-87. DOI: https://doi.org/10.1016/j.inffus.2020.12.008.
(113) Zhang, Z.; Cui, P.; Zhu, W. Deep Learning on Graphs: A Survey. *IEEE Trans. on Knowl. and Data Eng.* **2022**, *34* (1), 249–270 , numpages = 222. DOI: https://doi.org/10.1109/TKDE.2020.2981333.
(114) Chen, Y.; Chang, H.; Meng, J.; Zhang, D. Ensemble Neural Networks (ENN): A gradient-free stochastic method. *Neural Networks* **2019**, *110*, 170-185. DOI: https://doi.org/10.1016/j.neunet.2018.11.009.
(115) Jeong, H.; Oh, J.; Choi, Y.-L. GraphTME: a framework for predicting response to immune checkpoint inhibitors by interpreting cell-cell interactions in the tumor microenvironment using spatial transcriptomics of tumor tissue. *bioRxiv* **2025**, 2025.2007.2024.665835. DOI: https://doi.org/10.1101/2025.07.24.665835.
(116) Biancalani, T.; Scalia, G.; Buffoni, L.; Avasthi, R.; Lu, Z.; Sanger, A.; Tokcan, N.; Vanderburg, C. R.; Segerstolpe, Å.; Zhang, M.; et al. Deep learning and alignment of spatially resolved single-cell transcriptomes with Tangram. *Nat Methods* **2021**, *18* (11), 1352-1362. DOI:

https://doi.org/10.1038/s41592-021-01264-7.
(117) Xu, H.; Fu, H.; Long, Y.; Ang, K. S.; Sethi, R.; Chong, K.; Li, M.; Uddamvathanak, R.; Lee, H. K.; Ling, J.; et al. Unsupervised spatially embedded deep representation of spatial transcriptomics. *Genome Med* **2024**, *16* (1), 12. DOI: https://doi.org/10.1186/s13073-024-01283-x.
(118) Wang, Y.; Cao, G.; Zeng, H.; Zhi, Y.; Xu, M.; Wang, Y.; Liu, M.; Ruan, Y.; Tse, K. Y.; Zhang, Q.; et al. Multi-Omics Analysis Reveals the transforming growth factor-β Signaling-Driven Multicellular Interactions with Prognostic Relevance in Cervical Cancer Progression. *J Cancer* **2025**, *16* (9), 2857-2876. DOI: https://doi.org/10.7150/jca.114505.
(119) Guo, W.; Zhou, B.; Dou, L.; Guo, L.; Li, Y.; Qin, J.; Wang, Z.; Huai, Q.; Xue, X.; Li, Y.; et al. Single-cell RNA sequencing and spatial transcriptomics of esophageal squamous cell carcinoma with lymph node metastases. *Exp Mol Med* **2025**, *57* (1), 59-71. DOI: https://doi.org/10.1038/s12276-024-01369-x.
(120) LeCun, Y.; Bengio, Y. Convolutional Networks for Images, Speech, and Time Series," Handbook of Brain Theory and Neural Networks (M. Arbib, Ed.). MIT Press, Cambridge, Massachusetts: 1995.
(121) Baião, A. R.; Cai, Z.; Poulos, R. C.; Robinson, P. J.; Reddel, R. R.; Zhong, Q.; Vinga, S.; Gonçalves, E. A technical review of multi-omics data integration methods: from classical statistical to deep generative approaches. *Briefings in Bioinformatics* **2025**, *26* (4), bbaf355. DOI: https://doi.org/10.1093/bib/bbaf355.
(122) Korsunsky, I.; Millard, N.; Fan, J.; Slowikowski, K.; Zhang, F.; Wei, K.; Baglaenko, Y.; Brenner, M.; Loh, P.-r.; Raychaudhuri, S. Fast, sensitive and accurate integration of single-cell data with Harmony. *Nat Methods* **2019**, *16* (12), 1289-1296. DOI: https://doi.org/10.1038/s41592-019-0619-0.
(123) Stuart, T.; Butler, A.; Hoffman, P.; Hafemeister, C.; Papalexi, E.; Mauck, W. M.; Hao, Y.; Stoeckius, M.; Smibert, P.; Satija, R. Comprehensive Integration of Single-Cell Data. *Cell* **2019**, *177* (7). DOI: https://doi.org/10.1016/j.cell.2019.05.031.
(124) Fang, Z.; Krusen, K.; Priest, H.; Wang, M.; Kim, S.; Sriram, A.; Yellanki, A.; Singh, A.; Horwitz, E.; Coskun, A. F. Graph-Based 3-Dimensional Spatial Gene Neighborhood Networks of Single Cells in Gels and Tissues. *BME Front* **2025**, *6*, 0110. DOI: https://doi.org/10.34133/bmef.0110.
(125) Heitz, M.; Ma, Y.; Kubal, S.; Schiebinger, G. Spatial Transcriptomics Brings New Challenges and Opportunities for Trajectory Inference. *Annu Rev Biomed Data Sci* **2024**, *8* (1). DOI: https://doi.org/10.1146/annurev-biodatasci-040324-030052.
(126) Chen, R. T. Q.; Rubanova, Y.; Bettencourt, J.; Duvenaud, D. K. Neural Ordinary Differential Equations. In 2018.
(127) Tong, A.; Huang, J.; Wolf, G.; van Dijk, D.; Krishnaswamy, S. TrajectoryNet: A Dynamic Optimal Transport Network for Modeling Cellular Dynamics. *Proc Mach Learn Res* **2020**, *119*, 9526-9536.
(128) Hess, K.; Melnychuk, V.; Frauen, D.; Feuerriegel, S. Bayesian neural controlled differential equations for treatment effect estimation. *arXiv preprint arXiv:2310.17463* **2023**.
(129) Chen, Y.; Wang, D.; Li, Y.; Qi, L.; Si, W.; Bo, Y.; Chen, X.; Ye, Z.; Fan, H.; Liu, B.; et al. Spatiotemporal single-cell analysis decodes cellular dynamics underlying different responses to immunotherapy in colorectal cancer. *Cancer Cell* **2024**, *42* (7). DOI: https://doi.org/10.1016/j.ccell.2024.06.009.
(130) Moor, M.; Banerjee, O.; Abad, Z. S. H.; Krumholz, H. M.; Leskovec, J.; Topol, E. J.; Rajpurkar,

P. Foundation models for generalist medical artificial intelligence. *Nature* **2023**, *616* (7956), 259-265. DOI: https://doi.org/10.1038/s41586-023-05881-4.
(131) Wenckstern, J.; Jain, E.; Vasilev, K.; Pariset, M.; Wicki, A.; Gut, G.; Bunne, C. AI-powered virtual tissues from spatial proteomics for clinical diagnostics and biomedical discovery. *ArXiv* **2025**, *abs/2501.06039*.
(132) Park, J. E.; Eun, D.; Kim, H. S.; Lee, D. H.; Jang, R. W.; Kim, N. Generative adversarial network for glioblastoma ensures morphologic variations and improves diagnostic model for isocitrate dehydrogenase mutant type. *Sci Rep* **2021**, *11* (1), 9912. DOI: https://doi.org/10.1038/s41598-021-89477-w.
(133) Figiel, S.; Yin, W.; Doultsinos, D.; Erickson, A.; Poulose, N.; Singh, R.; Magnussen, A.; Anbarasan, T.; Teague, R.; He, M.; et al. Spatial transcriptomic analysis of virtual prostate biopsy reveals confounding effect of tissue heterogeneity on genomic signatures. *Mol Cancer* **2023**, *22* (1), 162. DOI: https://doi.org/10.1186/s12943-023-01863-2.
(134) Ho, J.; Jain, A.; Abbeel, P. Denoising diffusion probabilistic models. *Advances in neural information processing systems* **2020**, *33*, 6840-6851.
(135) Mirza, M.; Osindero, S. Conditional generative adversarial nets. *arXiv preprint arXiv:1411.1784* **2014**.
(136) Chowell, D.; Yoo, S.-K.; Valero, C.; Pastore, A.; Krishna, C.; Lee, M.; Hoen, D.; Shi, H.; Kelly, D. W.; Patel, N.; et al. Improved prediction of immune checkpoint blockade efficacy across multiple cancer types. *Nature Biotechnology* **2022**, *40* (4), 499-506. DOI: https://doi.org/10.1038/s41587-021-01070-8.
(137) Tang, J.; Fan, W.; Ruan, Y.; Liu, X.; Qiu, F.; Feng, J.; Huang, G.; Yan, M.; Wang, H.; Mu, Q.; et al. Protein-based classification reveals an immune-hot subtype in IDH mutant astrocytoma with worse prognosis. *Cancer Cell* **2025**. DOI: https://doi.org/10.1016/j.ccell.2025.08.006.
(138) Ji, G.-W.; Wang, K.; Xia, Y.-X.; Wang, J.-S.; Wang, X.-H.; Li, X.-C. Integrating Machine Learning and Tumor Immune Signature to Predict Oncologic Outcomes in Resected Biliary Tract Cancer. *Ann Surg Oncol* **2020**, *28* (7), 4018-4029. DOI: https://doi.org/10.1245/s10434-020-09374-w.
(139) Zinselmeyer, B. H.; Heydari, S.; Sacristán, C.; Nayak, D.; Cammer, M.; Herz, J.; Cheng, X.; Davis, S. J.; Dustin, M. L.; McGavern, D. B. PD-1 promotes immune exhaustion by inducing antiviral T cell motility paralysis. *J Exp Med* **2013**, *210* (4), 757-774. DOI: https://doi.org/10.1084/jem.20121416.
(140) Lin, Y.; Ma, J.; Yuan, H.; Chen, Z.; Xu, X.; Jiang, M.; Zhu, J.; Meng, W.; Qiu, W.; Liu, Y. Integrating Reinforcement Learning and Monte Carlo Tree Search for enhanced neoantigen vaccine design. *Briefings In Bioinformatics* **2024**, *25* (3). DOI: https://doi.org/10.1093/bib/bbae247.
(141) Schmucker, R.; Farina, G.; Faeder, J.; Fröhlich, F.; Saglam, A. S.; Sandholm, T. Combination treatment optimization using a pan-cancer pathway model. *PLoS Comput Biol* **2021**, *17* (12), e1009689. DOI: https://doi.org/10.1371/journal.pcbi.1009689.
(142) Eastman, B.; Przedborski, M.; Kohandel, M. Reinforcement learning derived chemotherapeutic schedules for robust patient-specific therapy. *Sci Rep* **2021**, *11* (1), 17882. DOI: https://doi.org/10.1038/s41598-021-97028-6.
(143) Bordukova, M.; Makarov, N.; Rodriguez-Esteban, R.; Schmich, F.; Menden, M. P. Generative artificial intelligence empowers digital twins in drug discovery and clinical trials. *Expert Opin Drug Discov* **2024**, *19* (1), 33-42. DOI:

https://doi.org/10.1080/17460441.2023.2273839.
(144) D'Amico, S.; Dall'Olio, D.; Sala, C.; Dall'Olio, L.; Sauta, E.; Zampini, M.; Asti, G.; Lanino, L.; Maggioni, G.; Campagna, A.; et al. Synthetic Data Generation by Artificial Intelligence to Accelerate Research and Precision Medicine in Hematology. *JCO Clin Cancer Inform* **2023**, *7*, e2300021. DOI: https://doi.org/10.1200/CCI.23.00021.
(145) Shen, S.; Qi, W.; Liu, X.; Zeng, J.; Li, S.; Zhu, X.; Dong, C.; Wang, B.; Shi, Y.; Yao, J.; et al. From virtual to reality: innovative practices of digital twins in tumor therapy. *Journal of Translational Medicine* **2025**, *23* (1), 348. DOI: https://doi.org/10.1186/s12967-025-06371-z.
(146) Ștefănigă, S. A.; Cordoș, A. A.; Ivascu, T.; Feier, C. V. I.; Muntean, C.; Stupinean, C. V.; Călinici, T.; Aluaș, M.; Bolboacă, S. D. Advancing Precision Oncology with Digital and Virtual Twins: A Scoping Review. *Cancers (Basel)* **2024**, *16* (22). DOI: https://doi.org/10.3390/cancers16223817.
(147) Reinoso-Burrows, J. C.; Toro, N.; Cortés-Carmona, M.; Pineda, F.; Henriquez, M.; Galleguillos Madrid, F. M. Cellular Automata Modeling as a Tool in Corrosion Management. *Materials (Basel)* **2023**, *16* (17). DOI: https://doi.org/10.3390/ma16176051.
(148) Sadhukhan, S.; Mishra, P. K.; Basu, S. K.; Mandal, J. K. A multi-scale agent-based model for avascular tumor growth. *Biosystems* **2021**, *206*, 104450. DOI: https://doi.org/10.1016/j.biosystems.2021.104450.
(149) Stephan, S.; Galland, S.; Labbani Narsis, O.; Shoji, K.; Vachenc, S.; Gerart, S.; Nicolle, C. Agent-based approaches for biological modeling in oncology: A literature review. *Artif Intell Med* **2024**, *152*, 102884. DOI: https://doi.org/10.1016/j.artmed.2024.102884.
(150) Thurber, G. M.; Reiner, T.; Yang, K. S.; Kohler, R. H.; Weissleder, R. Effect of small-molecule modification on single-cell pharmacokinetics of PARP inhibitors. *Mol Cancer Ther* **2014**, *13* (4), 986-995. DOI: https://doi.org/10.1158/1535-7163.MCT-13-0801.
(151) Bouriga, R.; Bailleux, C.; Gal, J.; Chamorey, E.; Mograbi, B.; Hannoun-Levi, J.-M.; Milano, G. Advances and critical aspects in cancer treatment development using digital twins. *Briefings in Bioinformatics* **2025**, *26* (3), bbaf237. DOI: https://doi.org/10.1093/bib/bbaf237.
(152) Jørgensen, A. C. S.; Ghosh, A.; Sturrock, M.; Shahrezaei, V. Efficient Bayesian inference for stochastic agent-based models. *PLoS Comput Biol* **2022**, *18* (10), e1009508. DOI: https://doi.org/10.1371/journal.pcbi.1009508.
(153) Jørgensen, A. C. S.; Hill, C. S.; Sturrock, M.; Tang, W.; Karamched, S. R.; Gorup, D.; Lythgoe, M. F.; Parrinello, S.; Marguerat, S.; Shahrezaei, V. Data-driven spatio-temporal modelling of glioblastoma. *R Soc Open Sci* **2023**, *10* (3), 221444. DOI: https://doi.org/10.1098/rsos.221444.
(154) Bai, L.; Su, J. Artificial Intelligence Virtual Organoids (AIVOs). *Bioactive Materials* **2026**, *59*, 45-68. DOI: https://doi.org/10.1016/j.bioactmat.2025.12.030.
(155) Yuan, Z.; Zhao, F.; Lin, S.; Zhao, Y.; Yao, J.; Cui, Y.; Zhang, X.-Y.; Zhao, Y. Benchmarking spatial clustering methods with spatially resolved transcriptomics data. *Nat Methods* **2024**, *21* (4), 712-722. DOI: https://doi.org/10.1038/s41592-024-02215-8.
(156) Knapp, A.; Cruz, D. A.; Mehrad, B.; Laubenbacher, R. C. Personalizing computational models to construct medical digital twins. *J R Soc Interface* **2025**, *22* (228), 20250055. DOI: https://doi.org/10.1098/rsif.2025.0055.
(157) Luecken, M. D.; Büttner, M.; Chaichoompu, K.; Danese, A.; Interlandi, M.; Mueller, M. F.; Strobl, D. C.; Zappia, L.; Dugas, M.; Colomé-Tatché, M.; et al. Benchmarking atlas-level data integration in single-cell genomics. *Nat Methods* **2022**, *19* (1), 41-50. DOI: https://doi.org/10.1038/s41592-021-01336-8.

(158) Karaman, I.; Sebin, B. From data-driven cities to data-driven tumors: dynamic digital twins for adaptive oncology. *Front Artif Intell* **2025**, *8*, 1624877. DOI: https://doi.org/10.3389/frai.2025.1624877.
(159) Kim, B. C.; Kim, B.; Hyun, Y. Investigation of out-of-distribution detection across various models and training methodologies. *Neural Netw* **2024**, *175*, 106288. DOI: https://doi.org/10.1016/j.neunet.2024.106288.
(160) Wang, X.; Lv, X.; Wang, J.; Zou, L.; Chen, Z.; Zhao, R.; Zhao, L.; Zhao, M.; Zhang, X.; Zhang, B.; et al. A multimodal uncertainty-aware AI system optimizes ovarian cancer risk assessment workflow. *npj Digital Medicine* **2025**, *8* (1), 614. DOI: https://doi.org/10.1038/s41746-025-01986-4.
(161) Bartusik-Aebisher, D.; Justin Raj, D. R.; Aebisher, D. Artificial Intelligence in Medical Diagnostics: Foundations, Clinical Applications, and Future Directions. In *Applied Sciences*, 2026; Vol. 16, p 728.
(162) Savage, S. R.; Yi, X.; Lei, J. T.; Wen, B.; Zhao, H.; Liao, Y.; Jaehnig, E. J.; Somes, L. K.; Shafer, P. W.; Lee, T. D.; et al. Pan-cancer proteogenomics expands the landscape of therapeutic targets. *Cell* **2024**, *187* (16). DOI: https://doi.org/10.1016/j.cell.2024.05.039.
(163) Wang, Y.; Bergman, D. R.; Trujillo, E.; Fernald, A. A.; Li, L.; Pearson, A. T.; Sweis, R. F.; Jackson, T. L. Agent-Based Modeling of Virtual Tumors Reveals the Critical Influence of Microenvironmental Complexity on Immunotherapy Efficacy. *Cancers (Basel)* **2024**, *16* (17), 2942.
(164) Kolokotroni, E.; Abler, D.; Ghosh, A.; Tzamali, E.; Grogan, J.; Georgiadi, E.; Büchler, P.; Radhakrishnan, R.; Byrne, H.; Sakkalis, V.; et al. A Multidisciplinary Hyper-Modeling Scheme in Personalized In Silico Oncology: Coupling Cell Kinetics with Metabolism, Signaling Networks, and Biomechanics as Plug-In Component Models of a Cancer Digital Twin. *J Pers Med* **2024**, *14* (5). DOI: https://doi.org/10.3390/jpm14050475.
(165) Park, S.-Y.; Kim, S.-J.; Park, C.-H.; Kim, J.; Lee, D.-Y. Data-driven prediction models for forecasting multistep ahead profiles of mammalian cell culture toward bioprocess digital twins. *Biotechnol Bioeng* **2023**, *120* (9), 2494-2508. DOI: https://doi.org/10.1002/bit.28405.
(166) Stahlberg, E. A.; Abdel-Rahman, M.; Aguilar, B.; Asadpoure, A.; Beckman, R. A.; Borkon, L. L.; Bryan, J. N.; Cebulla, C. M.; Chang, Y. H.; Chatterjee, A.; et al. Exploring approaches for predictive cancer patient digital twins: Opportunities for collaboration and innovation. *Front Digit Health* **2022**, *4*, 1007784. DOI: https://doi.org/10.3389/fdgth.2022.1007784.
(167) Wentzel, A.; Attia, S.; Zhang, X.; Canahuate, G.; Fuller, C. D.; Marai, G. E. DITTO: A Visual Digital Twin for Interventions and Temporal Treatment Outcomes in Head and Neck Cancer. *IEEE Transactions on Visualization and Computer Graphics* **2025**, *31* (1), 65-75. DOI: https://doi.org/10.1109/TVCG.2024.3456160.
(168) Chen, S.; Zhu, B.; Huang, S.; Hickey, J. W.; Lin, K. Z.; Snyder, M.; Greenleaf, W. J.; Nolan, G. P.; Zhang, N. R.; Ma, Z. Integration of spatial and single-cell data across modalities with weakly linked features. *Nature Biotechnology* **2024**, *42* (7), 1096-1106. DOI: https://doi.org/10.1038/s41587-023-01935-0.
(169) Wang, G.; Zhao, J.; Lin, Y.; Liu, T.; Zhao, Y.; Zhao, H. scMODAL: a general deep learning framework for comprehensive single-cell multi-omics data alignment with feature links. *Nature Communications* **2025**, *16* (1), 4994. DOI: https://doi.org/10.1038/s41467-025-60333-z.
(170) Görtz, M.; Brandl, C.; Nitschke, A.; Riediger, A.; Stromer, D.; Byczkowski, M.; Heuveline, V.; Weidemüller, M. Digital twins for personalized treatment in uro-oncology in the era of artificial

intelligence. *Nature Reviews Urology* **2026**, *23* (1), 29-39. DOI: https://doi.org/10.1038/s41585-025-01096-6.
(171) Bhardwaj, S.; Kumar, G.; Yang, H.; Bhardwaj, S.; Wang, Q.; Shen, M.; Wang, Y.; Souza, C. M. D. Virtual Cells: From Conceptual Frameworks to Biomedical Applications. 2025.
(172) Chen, F.; Li, Y.; Chen, Y.; Bian, Z.; Duo, L.; Zhou, Q.; Zhang, L.; Group, A. W. Strategies for the Analysis and Elimination of Hallucinations in Artificial Intelligence Generated Medical Knowledge. *Journal of Evidence-Based Medicine* **2025**, *18* (3), e70075. DOI: https://doi.org/10.1111/jebm.70075.
(173) Arunraju, C. Explainable AI (XAI) for trustworthy and transparent decision-making: A theoretical framework for AI interpretability. *World Journal of Advanced Engineering Technology and Sciences* **2025**, *14* (3), 170-207. DOI: https://doi.org/10.30574/wjaets.2025.14.3.0106.
(174) Adepoju, D. A.; Adepoju, A. G. Establishing ethical frameworks for scalable data engineering and governance in AI-driven healthcare systems. *International Journal of Research Publication and Reviews* **2025**, *6* (4), 8710-8726. DOI: https://doi.org/10.55248/gengpi.6.0425.1547.
(175) Yang, W.; Wei, Q.; Ma, C.; Tan, W.; Yan, B. Scaling Laws for Data-Efficient Visual Transfer Learning. *arXiv preprint arXiv:2504.13219* **2025**.
(176) Pan, R.; Sun, H.; Chen, X.; Pedrielli, G.; Huang, J. Human Digital Twin: Data, Models, Applications, and Challenges. *ArXiv* **2025**, *abs/2508.13138*.
(177) Hernandez-Boussard, T.; Macklin, P.; Greenspan, E. J.; Gryshuk, A. L.; Stahlberg, E.; Syeda-Mahmood, T.; Shmulevich, I. Digital twins for predictive oncology will be a paradigm shift for precision cancer care. *Nature Medicine* **2021**, *27* (12), 2065-2066. DOI: https://doi.org/10.1038/s41591-021-01558-5.